Spatial Distribution of Rat Oscillatory Potentials Evaluated using the Multi-Electrode Electroretinogram

BY
MARYAM HANIF
B.S., University of Illinois at Chicago, 2009

THESIS

Submitted as partial fulfillment of the requirements
for the degree of Masters of Science in Bioengineering
in the Graduate College of the
University of Illinois at Chicago, 2012

Chicago, Illinois

Defense Committee:

John R. Hetling, Chair and Advisor
Ali Djalilian, Ophthalmology and Visual Science
Jason McAnany, Ophthalmology and Visual Science
James Patton

This thesis is dedicated to my (late) grandmothers, Hamida Bai Hashim and Zubaida Bai.

ACKNOWLEDGEMENTS

I would like to thank, first and foremost, my parents, Shamim S. Hanif and Mohammad Hanif, and my uncles, Ashraf Dawood and Aftab Dawood, for their prayers and immense support.

I would like to thank my research advisor, Dr. John R. Hetling, for his advice and patience in helping me complete this project and for his guidance throughout my undergraduate and graduate education at the University of Illinois at Chicago (UIC).

I would like to thank my committee members, Dr. Ali Djalilian, Dr. John Hetling, Dr. Jason McAnany, and Dr. James Patton, for their helpful suggestions and recommendations.

I am indebted to some of the Neural Engineering Vision Lab (NEVL) members. I started this study by shadowing Ashley Selner (PhD Candidate), who provided her useful insight at the initial stages of my project. I would like to thank Hadi Tajalli (PhD Candidate) and Joel Thomas (PhD Candidate) for all the technical assistance they provided. Yelena Krakovaôs (Masters Candidate) contribution was crucial; I thank her for providing me raw data to work with and for patiently answering my many questions.

I would also like to thank some of the other Engineering students who provided their technical assistance in helping me complete this project; many thanks to Faezah Jahanmiri, Amit Shah, and Mahir Zakwan.

I would like to express my thanks to Dr. Richard Magin for his uplifting words and general support throughout my undergraduate and graduate education at UIC. I would also like to acknowledge Dr. David Eddington, with immense gratitude, for giving me the opportunity to do my very first research project in his lab.

Lastly, I would like to thank the institutions of UIC and Medtronic, Inc. for funding my Masterôs education through their generous fellowship, and for the opportunity to conduct research at the academic and industry level.

TABLE OF CONTENTS

LIST OF TABLES

LIST OF FIGURES

LIST OF ABBREVIATIONS

OP	oscillatory potential
meERG	multi-electrode electroretinogram
ERG	electroretinogram
IP	intrapertitoneal
SOP	sum of peaks
CME	cystoid macular edema
DR	diabetic retinopathy
MS	multiple sclerosis
CNS	central nervous system
PI	pancreatic insufficiency
PS	pancreatic sufficient
NEVL	Neural Engineering Vision Lab

SUMMARY

Oscillatory potentials (OPs) are a component of the corneal electroretinogram signal that reflects inner-retinal activity. Features of the OPs have been shown to be affected by disease states that involve changes in retinal circulation, such as diabetic retinopathy or retinopathy of prematurity. The multi-electrode electroretinogram (meERG) is a developing technique which records ERG potentials at several locations on the cornea simultaneously, with the promise of detecting regional dysfunction at the retina. The goal of this study was to characterize oscillatory potential (OP) amplitudes as a function of location on the cornea, in Long-Evans rats. Variation of OPs across electrode positions and radial eccentricity were analyzed, and variances of repeated measures across animals were evaluated for nine rats at 6 and 7 weeks of age.

Specific Aim 1 ï OP amplitudes across electrode positions were analyzed. The spatial variance of the OP amplitudes was found to be typically in the range of 10-30% of the mean amplitude, and was typically smaller than the spatial variance of the a-wave and b-wave amplitudes in the same responses. This may imply a different spatial distribution of the cell types that give rise to these three components.

Specific Aim 2 ï Variation of OP amplitudes as a function of radial eccentricity on the cornea was examined. The SOP amplitudes were found to be similar between the A, B, C and M rings, consistent with the low spatial variance described under Specific Aim 1.

Specific Aim 3 ï The variation of OP amplitudes between animals was evaluated. Large differences in mean OP amplitudes were found, similar to between-animal differences found in other ERG components. The utility of the meERG approach lies in the ability to

measure spatial differences within an animal, so between-animal differences in mean amplitudes are not a challenge to this approach.

Specific Aim 4 ï Variation of OP amplitudes for repeated measures was examined. Significant differences were found in OP amplitudes for the same test performed one week apart in the same animal, but relative spatial differences were preserved.

I. Introduction

1. Problem Statement:

1.1. Oscillatory potentials (OPs) are a component of the corneal electroretinogram signal that reflect inner-retinal activity. Features of the OPs have been shown to be affected by disease states that involve changes in retinal circulation, such as diabetic retinopathy or retinopathy of prematurity. The multi-electrode electroretinogram (meERG) is a developing technique which records ERG potentials at several locations on the cornea simultaneously, with the promise of detecting regional dysfunction at the retina. A main objective of the Neural Engineering Vision Laboratory (NEVL) at UIC is to evaluate the potential applications of meERG recording in clinical detection, diagnosis and monitoring of eye disease.

2. Gap in knowledge:

2.1. In response to a visual stimulus, neurons of the retina change their membrane potential, leading to local extracellular currents. The passing of current through the extracellular space of the retina results in extracellular field potentials, collectively known as the electroretinogram (ERG). The distribution of these bioelectric potentials can be represented as dipoles, resulting in a positive potential at some depths of the retina and negative at others. Change in magnitude of the current with the depth in the retina implies variation in vertical orientation of the cell type at which the current was generated. This method of analyzing cellular origins, known as current source density analysis, allows assessment of the cellular origin (at vertically depth) in the retina. (Karwoski et al., 1996). In contrast, the meERG has the potential to analyze the spatial distribution of cellular activity in lateral direction, which c ould be used to assess damage

to different spatial locations of the retina, for disease detection or monitoring. Variation in magnitude or polarity of the recorded ERG across the cornea is related to alteration of cellular current across the retina (Cringle et al., 1986).

While the meERG technique is being developed for clinical use, a great deal can be learned in animal studies. For example, there are several rat models of human eye disease, including diabetic retinopathy (Layton et al., 2007; Fernandez et al., 2011) and retinopathy of prematurity (Liu et al., 2006; Akula et al., 2007). Understanding the spatial distribution of OPôs, as revealed by meERG recording in healthy rats, is an essential first step toward optimizing this measurement for the study or diagnosis of important eye diseases which may be associated with pathologic changes in OP features. Characterizing variance of normative data would allow differentiating disease state and óabnormalô data. The work described in this thesis focused on the oscillatory potentials recorded in normally-sighted rats; this ERG component has never, to the authorôs knowledge, been evaluated as a function of position on the cornea.

2.2. Description of Specific Aims:

2.2.1. Overall Goal: To characterize oscillatory potential (OP) amplitudes as a function of location on the cornea in normally sighted rats.

2.2.1.1. Specific Aim 1 ï Analyze variation of OP amplitudes across electrode positions in individual meERG responses. The variance at a single flash strength will be characterized in three animals.

2.2.1.2. Specific Aim 2 – Analyze variation of OP amplitudes as a function of radial eccentricity on the cornea. Differences between ñringsò will be described for highest flash strength, 159 sc cd s/m^2, for three animals.

2.2.1.3. Specific Aim 3 – Analyze variation of OP amplitudes between animals. Mean amplitudes of individual OP peaks and sum of peaks, at each degree of corneal eccentricity (ñringsò), will be evaluated.

2.2.1.4. Specific Aim 4 ï Analyze variation of OP amplitudes for repeated measures (one week apart) on the same animals.

Additional analysis was performed to compare OPs isolated from meERG data to published reports of OPs recorded with conventional ERG. Variation of latencies of OP amplitudes was evaluated as a function of stimulus strength, as well as the dependence of OP amplitude on stimulus strength was analyzed.

2.3. Summary of results:

Specific Aim 1 ï OP amplitudes across electrode positions were analyzed.

- Variance typically in the range of 10-30% of the mean
- Variance typically smaller than the variance of the a- and b-wave amplitudes
- May imply a different spatial distribution of the origins of each component

Specific Aim 2 ï OP amplitudes as a function of radial eccentricity on the cornea was examined.

- Amplitudes were found to be similar between the A, B, C and M rings

Specific Aim 3 ï OP amplitudes between animals were evaluated.

- Large differences were found, similar to other ERG components
- Spatial differences within an animal are the core of this approach

Specific Aim 4 ï OP amplitudes for repeated measures were examined.

- Significant differences were found between test performed one week apart
- Relative spatial differences were preserved

II. Background

A. Description of meERG recording technology:

The multi-electrode electroretinogram (meERG), a non-invasive technique created at the Neural Engineering Vision Laboratory at UIC, is being developed as a measure of localized retinal damage. It provides a map of bioelectric potentials at several locations on the cornea. This technique could be used as an early detection tool for many eye diseases, including diabetic retinopathy, age-related macular degeneration, retinopathy of prematurity, glaucoma and retinitis pigmentosa, among others.

The meERG is recorded with a contact lens electrode array (CLEAr LensÊ) made primarily of PMMA (poly methyl methacrylate), which is fabricated to conform to the curvature of the cornea. For human studies, the CLEAr LensÊ has a 33-channel electrode array. This study was done with a rat adapted CLEAr LensÊ that had a 25-channel electrode array. Compared with existing technology for mapping retinal function (mfERG, HVF), the CLEAr LensÊ provides a direct physiological measure, allows for shorter test duration, sensitivity to peripheral damage, and does not require the patient to have good visual acuity or to fixate on a small visual target.

The multi-focal electroretinogram (mfERG) uses a pattern stimulus to derive correlation between responses from the retina and stimulus location. Some of its limitations, compared to the meERG, are that it requires the patient to have a sharp focus of the pattern stimulus, and fixate on a small target, which may be difficult for patients with low central vision, and poor visual acuity. It is an indirect measure of the cell5 responses, restricted to a limited area of the retina, and primarily measures response from the cones. Another test used to measure retinal response is the Humphrey Visual Field

Test, which is a psychophysical assessment of the visual response. It is not a physiological measure of visual function, and requires a patient to fixate on a small target and depends on the patient to response (pressing a button), to asses sensitivity of the central retina.

B. Other meERG studies in NEVL

To help put the contribution of this thesis into a broader context, the following summary of other meERG-related research activities in the NEVL is provided.

The overall meERG research project has been in progress for approximately six years. Two major lines of early-stage research are being pursued: CLEAr LensÊ development and meERG recording in human subjects, and CLEAr LensÊ development and meERG recording in rats. In both human and rat studies, the first aims have been to increase the yield of functional recording channels of the CLEAr Lenses, and to perform early characterization of the meERG signal, including establishment of the first normative data sets. More advanced work that is being performed in parallel is the creation, optimization and validation of finite-element models of the rat and human eyes. These models will eventually be used to solve the inverse problem, using meERG recorded potentials to predict the distribution of activity in the retina. The NEVL is also involved in translational science, having obtained two issued patents which are currently under exclusive option by a start-up company founded by lab alumni. Additional work being performed includes obtaining proof of concept for variations in the spatial distribution of meERG potentials due to changes in the spatial distribution of the retinal response. In rats, this is being accomplished using a laser-damage model to create local scotomas (blind spots); in human subjects, this is being accomplished by recruiting

patients with well-defined scotomas in an on-going study performed in collaboration with the Chicago Lighthouse for the Blind and Visually Impaired.

C. Anatomy of the Retina

The cornea is located at the front of the eye and is involved in refracting light, along with the lens, to create a focused image at the retina. The retina lines the back of the eye and contains the light sensitive cells, the rods and cones. It is the part of the eye where image processing occurs, in which the light rays are converted into impulses that are sent to the brain (to be interpreted) through the optic nerve. **Figure1** gives a schematic diagram of the retina. Light enters the retina through the inner limiting membrane. The ganglion cell layer (GCL), which consists of ganglion cells, forms the inner most part of the retina; which is followed by the inner nuclear layer (INL), which consists of amacrine cells, bipolar cells and horizontal cells. Further back into the retina is the outer nuclear layer (ONL), which consists of the rod and cone cell bodies. The inner plexiform layer (IPL) and the outer plexiform layer (OPL), consists of the various cell synaptic junctions. The most distal part of the retina consists of the rods and cones.

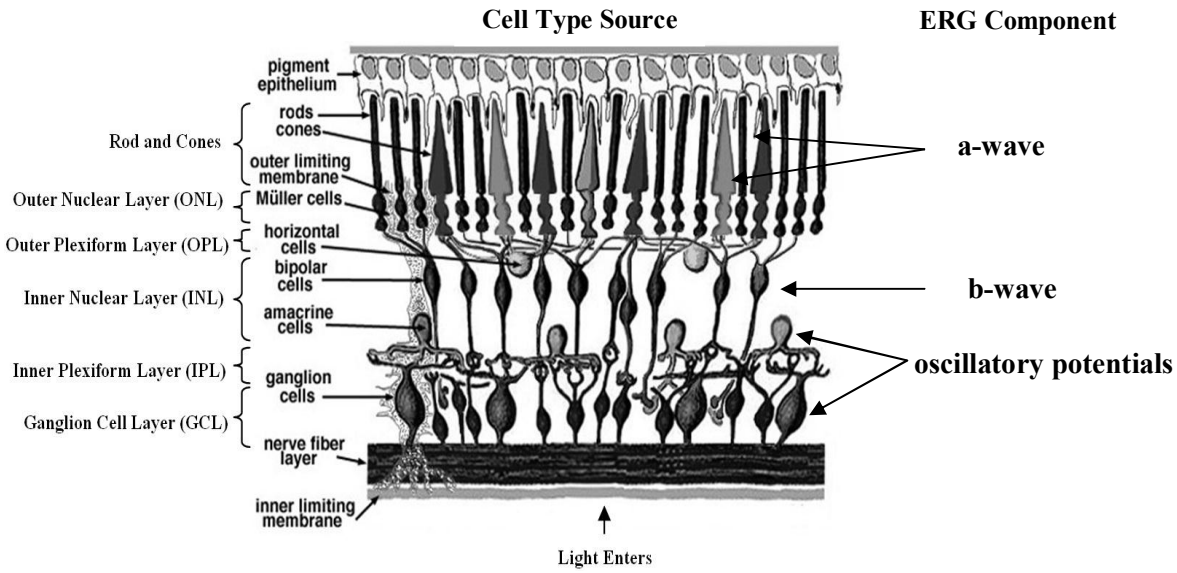

Figure 1 Schematic diagram of the organization of the retina (Source: webvision.med.utah.edu) and the associated ERG components.

D. Origins of major ERG components

Bioelectric potentials of the retina, evoked by light exposure, are collectively known as the ERG (electroretinogram), which comprises several major components: a-wave, b-wave, and oscillatory potentials (OPs). **Figure 2** depicts an ERG and its major components.

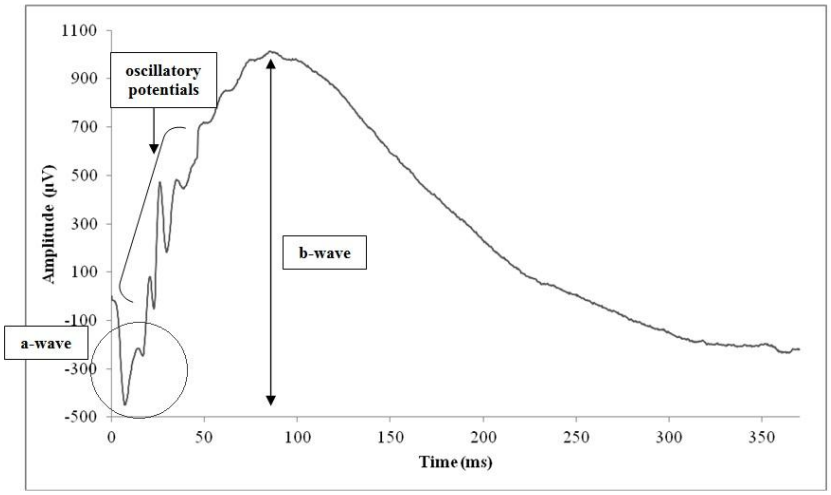

Figure 2 Electroretinogram (ERG) and its major components ï a-wave (large initial negative potential), b-wave (large positive peak), and oscillatory potentials (series of peaks on the rising edge of the b-wave).

Cellular origins of the major ERG response components can be analyzed using a technique known as current source density analysis, which identifies localized current sources and sinks at different depths of the retina, by measuring both voltage and resistance information. Field potentials are transmembrane currents associated with

intracellular hyperpolarization and depolarization, where the current entering extracellular space is the source and exiting the extracellular pace is the sink (Karwoski et al., 1996).

A second method to analyze the contribution of the different cell types is known as pharmacological dissection. In this method, different pharmacological agents are used to block activity of specific retinal cells, and depending on the agent the response of the remaining unaffected cells can be examined or the obstructed response of the block cell can be examined (Xu et al., 2003).

i. **a-wave**: A strong stimulus in scotopic setting (in which the eye is dark adapted), results in a rod driven negative wave; in a photopic setting (in which the eye is light adapted), it is cone driven, when the rods are saturated (Frishman, 2005). In response to a weak stimulus, the scotopic threshold response (STR) is visible, which is different from the a-wave. Hood (1990) has classified the a-wave response to be related to photoreceptors. Hood et al. (2002) investigated the cellular origins of the ERG using the TTX to block sodium channels, which allowed elimination of the inner retinal contributions. By removing this contribution, it allowed for analysis of the ON and OFF bipolar cellsô contribution to the ERG. It was reported that the hyperpolarization of the OFF bipolar cells resulted in the generation of the negative potential, N1 (a-wave). It was also reported that the photoreceptors also contributed to the generation of the N1, though the contribution was small (Hood et al., 2002).

ii. **b-wave**: The most prominent component of the ERG is the large positive peak, labeled as the b-wave. These have been generalized to occur in response to depolarization of the ON bipolar pathway (Hood and Birch, 1996), though they may

occur in the bipolar cell synaptic layer (Ruether et al., 2000). Hood et al. (2002) noted that the generation of the major positive component, P1 (b-wave), had a large contribution from the depolarization of the ON bipolar cells and a small contribution from the recovery of the OFF bipolar cells.

The generation of the b-wave has been reported to be affected by the oscillatory potentials (Lachapelle, 1990; Layton et al., 2007). Layton et al. (2007) investigated the effect of streptozotocin induced diabetes on b-waves and OPs. Not only did dark adaptation of the ratsô eyes increase the amplitude of b-waves and OPs in normal rats, the rats with induced diabetes showed decreased amplitudes and increased peak times for both ERG components. An OP constant was also generated, that represented a linear relationship between the b-wave and the OPs. With increase in duration of the diabetes state, this constant was seen to decrease linearly, indicating a loss in correlation of the OPs and b-waves with progressive disease state. It was further explained that the inconsistencies in studies regarding b-waves could be due to the OPs masking the b-wave (Layton et al., 2007).

iii. **Oscillatory potentials**: One of the first studies to report the OPs were done by Cobb and Morton (1953); they reported seeing four to six peaks superimposed on the rising edge of the b-wave, which were of uniform amplitude. They also reported seeing the OPs and the b-waves in humans disappeared when temporary blindness was induced by applying local pressure to the eye. Furthermore, under anoxic conditions they were able to determine that the origin of the OPs was different from the a-wave and the b-wave.

The origin of oscillatory potentials is a highly debated topic. One of the earliest studies, to identify the origins of OPs, reported that the earlier OP peaks may be generated near the retinal ganglion cells, in the proximal retina, while the latter OP peaks were generated near the photoreceptors in the distal retina (Wachtmeister and Dowling, 1978). Other sources of origin have been reported to be, inner plexiform layer (Fortune et al., 2002), OFF retinal pathway (Kojima et al., 1978), ganglion cells (Steinberg, 1966), amacrine cells (Wachtmeister and Dowling, 1978), and bipolar cells (Kaneko, 1970).

Nakamura et al. (2012) conducted a morphological study of the oxygen induced retinopathy state rat retina, by studying the cell number in the ganglion cell layer, the inner plexiform layer, inner nuclear layer, outer plexiform layer, and the outer nuclear layer. They reported seeing no correlation between the attenuation of the a-wave and the b-wave with the structural degeneration. They saw a significant decrease in the inner plexiform layer and the inner nuclear layer in disease state rats. Because amacrine cells form a big part of the inner plexiform layer, it was reported that this thinning of the layers could be due to lesions to the amacrine cells; this was correlated to the decrease in OP amplitudes. It was further reported that the there was a decrease in capillary density, which is also correlated to the attenuation in OP amplitude, and may be indicative of blood retina barrier disruption and symptoms of retinal vascular abnormalities (Nakamura et al., 2012).

E. Oscillatory potentials in disease states

1. *Retinopathy of Prematurity (and OPs in infants)* ï Zhou et al. (2010) reported seeing less frequent OPs in healthy preterm babies, (whose ERGs were recorded at birth), compared to babies born at due date and babies at 4 weeks of age. Furthermore, it was

noted that OPs are most immature part of the ERG, but also the most rapidly developing ERG response. Westall et al. (1999) reported seeing OPs in infants mature as fast as reaching adult level OPs by 2 years of age. They further described that the difference between OPs of an infant and a 16 year old is far greater than the difference between b-waves of the two age groups; suggesting that the slowly maturing OPs are dependent on the maturation of the visual mechanism. Another study (Moskowitz et al., 2005) compared the OPs of 10 week old infants with adults in scotopic and photopic conditions. They reported not seeing any significant different between scotopic and photopic OPs of infants, however, the difference for adults was quite large; the photopic OPs were significantly greater in amplitude than scotopic OPs. When scotopic OPs were compared between the two age groups, the infants had smaller OP amplitudes than the adults; a similar response was seen for photopic OPs between the age groups as well, but there was no correlation reported between the age and the number of photopic OP peaks.

Blood vessels begin developing in a fetus at 3 months and continue to develop till birth. Retinopathy of Prematurity (ROP) develops in premature births, when process is disrupted and the blood vessels grow abnormally or stop growing, resulting in blood leakage in the eye (ADAM Medical Encyclopedia). Fulton et. al (1996) have reported correlation between abnormal OPs and ROP. In an analysis of animal models of healthy rats and rats with oxygen induced retinopathy, it was reported that each OP peak in the signal is significantly attenuated, except for OP5, which was similar for both (Liu et al., 2006). It was also noted that with increasing stimulus strength, the OP amplitudes increased and there was a decrease in their implicit time.

Akula et al. (2007) used another approach to analyze OPs in the animal ROP models and humans; utilizing the œenergyô (E) of OPs, which is related to the square of SOP amplitudes, and is a function of the power (P) of the peaks and the frequency at the Gaussian model peak. It was reported that there was a difference in ROP effect on OPs, in rat models and humans. Rats that were induced ROP 50%/10% oxygen levels showed delayed OPs which had smaller amplitudes and lower energy, when compared to control rats. A similar OP response was seen in rat models with 75% oxygen exposure, but they showed more sensitivity than control rats. In humans however, it was seen that adults with a history of ROP had lower OP energy than control adults, but this was opposite in infants; infants with a history of ROP were reported to have greater OP energy than control infants.

Because even after a depreciation in ROP conditions, the retinal function does not fully return to normal, further analysis of morphological and functional changes due to ROP were analyzed by Nakamura et al. (2012). It was reported that the mice models with retinopathy, at 4, 6 and 8 weeks of age had approximately 50% decrease in OP amplitudes than the controls. In an analysis of physical retinal damage, a decrease in thickness of the inner plexiform layer, outer plexiform layer, and the inner nuclear layer was reported. However, compared to the control mice, the thickness of the outer nuclear layer and the number of cells in the ganglion cell layer was not significantly different.

2. *Diabetic Retinopathy* ï Diabetic patients, who have fairly uncontrolled blood sugar levels, develop damage to the blood vessels in the retina, causing loss of vision (ADAM Medical Encyclopedia). Vandala et al. (2002) did a long term study of OP analysis in diabetic patients with insulin dependence. At the conclusion of their 10 year

study, they reported that about half (46%) the diabetics with developing retinopathy had reduced OPs, and 75% of the diabetic patients who had normal fundus also had normal OP amplitudes. Furthermore, it was concluded from this long term study that the patients with normal fundus who showed reduced OPs developed diabetic retinopathy (DR) earlier, than those who did not show a reduction in OPs.

Kizawa et al. (2006) conducted a study comparing the different stages of severity of DR. Even though no significant variability was seen for the a-wave, the b-wave and the OPs were attenuated even for mild DR, and the OPs were delayed with increasing severity; in addition, the ration of SOPs/b-wave was also delayed with progressive retinopathy. Comparing the clinical significance of OPS to photopic negative response of the ERG, they found OP to be a more sensitive measure of detecting early staged of DR.

This was similar to Layton et al.ôs (2007) rat model, and Movasat et al.ôs (2008) human study findings, that the implicit time of OPs was significantly prolonged and amplitude attenuated, which could be indicative of the alterations in sensitivity of the inner retinal layer. However, Movasat et al. (2008) report the affect on only OP1 and that OP2 and OP3 were fairly unaffected by diabetes, but the SOP amplitude of diabetics was much lower than the control. In contrast, Luu et al. (2010), found all OPs (OP1-OP4) to have attenuated amplitude and prolonged implicit time in rod driven response, for diabetic patients. In addition, they also reported seeing a correlation between OP4 amplitude and vascular dysfunction. Vessey et al. (2011), also saw the significance of OP4 in the C57BL/6 mice, (not conclusive if this is the same OP4 as Luu et al., 2010) in their study; they too reported a significant attenuation of OP3 and OP4 amplitudes in their mice model, indicative of alterations in the inner retinal layer, but OP2 was

uncompromised in the disease model compared to the control. In addition, just as was reported by Nakamura et al. (2012), Vessey et al. (2011), also saw depreciation in the thickness of the inner nuclear layer and the inner plexiform layer, in the retinopathy model.

As seen with some of the studies above, generally the effect of diabetes in animal models and human studies is attenuation in amplitude of the OPs and an increase in their implicit time. However, it may be that multiple disease states may cause variations in that generalization. Huber et al. (2011) investigated type 2 diabetic rat models, who were also hypertensive and obese. Their findings showed that this model had a significant delay in OP implicit time; however, there was no significant attenuation of amplitude. Not only can OPs be utilized to study diabetes with other disease states, it may also be used to study treatments and preventative measures. It is reported that the use ischemic pulses as a method of preconditioning the eye against ischemic injury prevented reduction in SOP amplitudes, compared to rats without the conditioning, which had a significant decline in amplitude after 9 weeks of diabetes onset (Fernandez et al., 2011).

3. *Glaucoma* ï damage to the optic nerve, which carries information from the visual system to the brain, occurs due to increased intraocular pressure (ADAM Medical Encyclopedia). mfERG analysis on macaque monkeys have been reported to generate two distinct frequencies of OPs, fast (~143 Hz) and slow (~77 Hz) (Rangaswamy et al., 2006). The slow frequencies, which are extracted with a 90 - 300 Hz filter, and have the largest OP RMS (root mean square) amplitude in the foveal region, are the most commonly cited OPs with flash ERG; in glaucoma models, these have seen to be largely reduced in amplitude (Rangswamy et al., 2006). In a rat model of Glaucoma, it was

reported that the amplitudes of scotopic and photopic OPs, as well as photopic b-wave was significantly attenuated, signifying a loss of ganglion cells, but no prolonged implicit times were noted (Heiduschka et al., 2010). In scotopic ERG, the reduction of OP amplitude in Glaucoma models has been reported to emerge as early as 20 days after the disease induction (Bayer et al., 2001). Also in human patients, with high tension primary open angle glaucoma and normal tension glaucoma, the OP components were diminished in disease state subjects, compared to the control (Nork et al., 2000; Fortune et al., 2002; Heiduschka et al., 2010). Furthermore, loss and impairment of photoreceptors was reported in Glaucoma subjects (Nork et al., 2000; Heiduschka et al., 2010).

4. *Retinitis Pigmentosa* ï a genetic disorder in which the mostly the rods degenerate, leading to loss of vision in the periphery of the eye and night blindness (A.D.A.M. Medical Encyclopedia). Ikenoya et al. (2007) assessed OPs in patients with early stage retinitis pigmentosa (RP), using focal macular electroretinogram and varying stimulus spot sizes. It was reported that OP amplitudes for stimulus spot size of 5° was too small even in normal eyes to be calculated. It was reported that the OPs are preserved in RP, compared to the a-wave and the b-wave. In addition, the degree at which the amplitude of the ERG components attenuated increased with enlarging stimulus spot size (Ikenoya et al., 2007). Burnstedt et al., (2008) studied the full field ERG of retinitis pigmentosa patients with Bothnia dystrophy, a recessive gene mutation. One eye of the each patient underwent 24 hours of dark adaptation. It was reported that the sum of peaks of the OPs increased after the dark adaptation, and in the youngest patient reaching normal levels, indicating scotopic and photopic activity resulting in OPs (Burnstedt et al., 2008).

5. Other OP research:

5.1 *Cystoid Macular Edema* ï usually occurring after a cataract surgery, the macula, which is responsible for the central vision, swells up due to fluid leakage from the blood vessels in the retina and cause vision loss (Kellogg Eye Center). Not many studies have been reported that analyze OPs to assess retinal function in patients with cystoid macular edema (CME). Miyake et al. (1993) was one of the first studies to assess the OPs in patients with cystoid macular edema. They found that the patients with different visual acuities still saw a reduction in the amplitudes of the OPs, along with amplitude reduction in a-wave and b-wave. Terasaki et al. (2003) also had similar findings. They assessed OPs from full-field ERGs, in patients with aphakic and pseudophakic CME, and found the mean sum of peaks of the OPs to be significantly reduced, and the implicit times of these peaks were significantly delayed. Furthermore, this attenuation was strongly correlated with visual acuity of these patients. In addition, similar to Miyake et al. (1993), they found no statistically significant reduction in amplitudes of a-waves and b-waves of patients with CME.

5.2 *Myopia* ï refractive error which causes distant objects to be blurred. The OPs have previously been used to asses diseases in the retina and predict rod-cone interactions, (Lei et al., 2006); it would be beneficial to study OPs to investigate developing myopia in patients. Chen et al. (2006) studied OPs in human adults with myopia, using slow flash multifocal ERG. It was reported, that 3 OP peaks were obtained and the OP amplitudes, but not their implicit times, varied with retinal location. When the emmetropes, stable myopes, and progressing myopes were compared, it was found that OP2 and OP3 had shorter implicit times in progressing myopes, compared to the other

two groups. However, the OP amplitudes showed no statistically significant differences amongst the groups.

5.3 *Effect of Cigarettes* ï Cigarette smoking has been known to be detrimental to health, including having several carcinogenic chemicals. Furthermore, smoking has been linked to worsen symptoms in many disease states. Some of the first studies that evaluated the effects of cigarette smoking on the eye using an ERG focused on the a-wave (Gundogan et al., 2007), and the b-wave (Ingenito, 1979; Leighton et al., 1979; Gundogan et al., 2007). A recent study conducted by Varghese et al. (2011) evaluated the effect of nicotine on the ERG response, by administering different dosages of nicotine gum to healthy, non-smoking subjects. In the dark adapted setting, a statistically significant decrease in normalized b-wave amplitude was reported, for both administered dosages of nicotine, but no significant affect in amplitude and implicit time for neither the a-wave, nor the oscillatory potentials. In the light adapted ERG recordings, the 4mg dosage of nicotine gum resulted in increase in the b-wave amplitude. Similar to the dark-adaption, no significant affect was observed by them in the a-wave and the OPs.

5.4 *Age-related changes* ï Kergoat et al. (2001) analyzed OPs in adults, 75 and older, using flash ERG to evaluate the alterations in the inner plexiform layer of the retina, due to age. It was found, that compared to the younger subjects group, the a-wave and the b-wave was reduced in the older subjects for both the blue flash and white flash stimulus. It was also found that three OP peaks were generated with the blue flash stimulus, five peaks with white flash stimulus and four peaks with red flash stimulus. They reported having amplitudes of OP peaks in all stimuli to be attenuated in the older

group, except OP5 in white flash and OP4 in red flash. It was further reported that implicit times of the OP peaks, under all three stimuli was prolonged.

Age-related macular degeneration (AMD), usually occurring in people 50 and older, is degeneration in the macula, which causes loss of central vision (National Eye Institute). Walters et al. (1999) analyzed the effect on the ERG response due to AMD; they reported a significant reduction in the amplitudes of the b-wave and OP peak 2. They did not report further analysis on the effect of AMD on other OP peaks, which could be indicative of the fact that AMD does not significantly affect the other OP peaks.

5.5 *Cystic Fibrosis* ï a genetic disease which causes mucus build-up in lungs, pancreas, digestive tract and other parts of the body (ADAM Medical Encyclopedia). MS patients with pancreatic insufficiency may have vitamin A deficiency; Suttle et al. (1998) linked this vitamin A deficiency to ERG abnormalities. OôDonnell and Talbot (1987) reported in a case study that supplementing vitamin A may improve some visual function, and the b-wave that was originally attenuated in the patient returned to normal amplitude. Whatham et al. (2009) compared pancreatic sufficient (PS) MS patients to patients with pancreatic insufficiency (PI), who were administered vitamin A, B carotene, and retinol binding protein (RBP). They reported having no significant difference in the OP amplitudes and implicit times, measured from PI and PS patients, which is indicative of adequate nutrient supplementation in the PI group.

5.6 *Multiple Sclerosis (MS)* ï an auto-immune disease that may be caused by a virus or a defective gene, in which the myelin sheaths of the nerve cells are damaged, causing inflammation and affecting the brain and the central nervous system

(CNS) (ADAM Medical Encyclopedia). Studies have shown the presence of retinal antigen antibodies in MS patients (Gorczya et al., 2004) and MS patients with auto immune retinopathy (Forooghian et al., 2003). Forooghian et al. (2006) further investigated retinal autoimmunity in MS patients. It was found that the photopic OPs in patients with MS had a decrease in amplitudes, along with an increase in the implicit times of rod-cone b-waves, the cone b-waves, and the a-waves of the bright flash response. It was further shown that the MS patients with high anti-retinal antibodies had a decrease in photopic OP sum amplitudes, and delay in the implicit time of the rod-cone b-wave.

III. METHODS

A. Experimental design:

Due to the focus of this project being on collecting normative meERG data from rat, there is no set hypothesis, controls or independent variables. Long-Evans rats were used in this study. The animals (n=9) were tested at 6 and 7 weeks of age; they weighed between 200-250 g at 6 weeks of age and between 250-310 g at 7 weeks of age. This age range was chosen for best fit of the CLEAr LensÊ to the rat eye.

B. Experimental protocol:

The data was collected with a 25-electrode rat adapted CLEAr LensÊ . **Figure 3: A** gives the experimental setup of the lens on the rat eye. **Figure 3: B** gives a schematic of the arrangement of the electrodes on the lens, which was placed on the cornea. The 25 electrodes are arranged in 3 concentric rings, A ring, B ring, C ring, and a middle electrode (M); 12 electrodes form the A ring, 8 electrodes form the B ring and 4 electrodes form the C ring. Prior to the lens fitting, the rat was dark adapted for 1 hour. The rat was then anesthetized with 100 mg/kg concentration of ketamine and 5 mg/kg concentration of xylazine (IP). The pupil was dilated with 1% tropicamide, and 2.5% phenylephrine, and the cornea was anesthetized with 0.5% propacaine. The lens was filled with a saline solution and fitted to the rat eye. The responses were recorded over a stimulus range of 0.01 ï 159 scotopic candela seconds per meters^2 (sc cd s/m^2), using MC-Rack software, (Multi Channel Systems, Germany). The sampling rate was 5 kHz. Four to five responses per flash strength were recorded and averaged for analysis. For the purposes of this study, the average of the 4-5 responses will be represented as one recording.

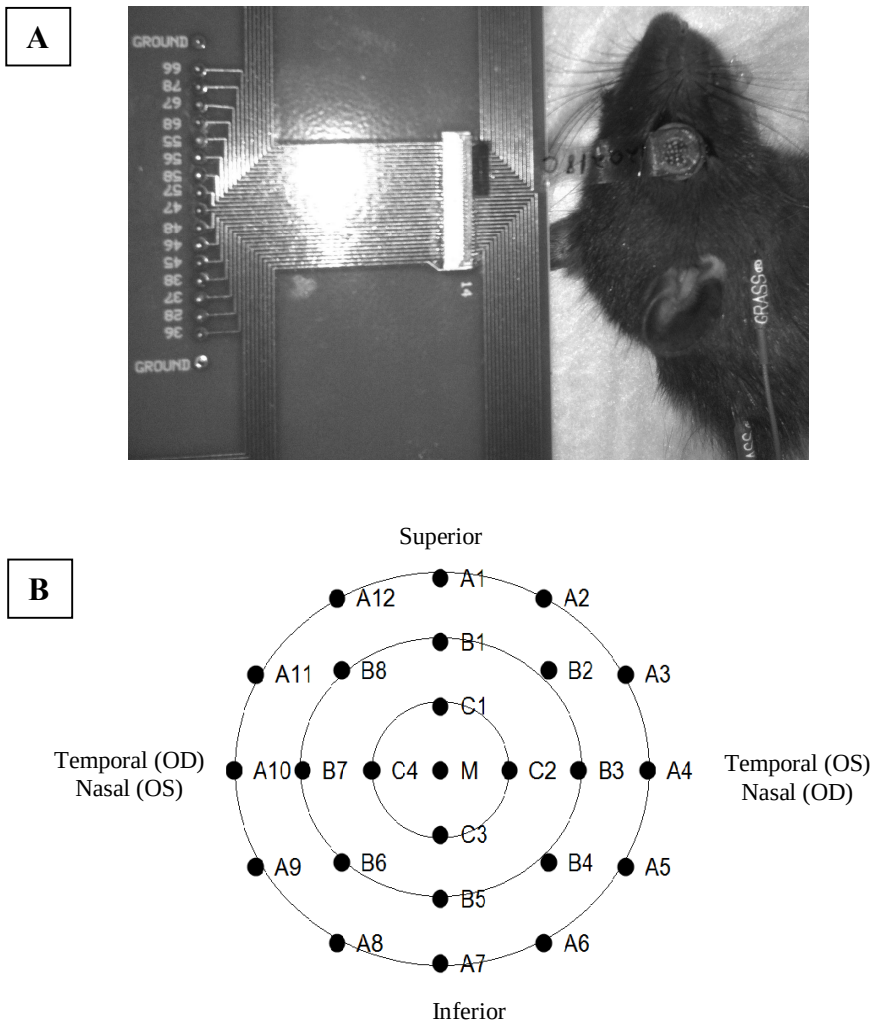

Figure 3 A) Lens placement on the rat cornea. During setup and experimentation, the lens may not exactly be aligned to the schematic of the lens. (Image courtesy of Hadi Tajalli) B) Schematic of placement of electrodes on the rat cornea. 25 electrodes are aligned in 3 concentric rings, A ring, B ring, C ring and a middle electrode.

C. Analysis tools:

a. Extraction of oscillatory potentials: The OPs were extracted using the ISCEV guidelines for dark-adapted oscillatory potentials (Marmor et al., 2009). The protocol recommends using a flash stimulus of 3.0 sc cd s/m^2 for humans. Multiple flash

strength stimuli were used to assess the OPs, in this study. Marmor et al. (2009) recommend highpass filtering the ERG signal between 75 - 100 Hz and lowpass filtering at 300 Hz or higher. The OPs were extracted using MATLAB (The Mathworks, Inc.), using a 4^{th} order Butterworth filter with a lowpass cutoff of 300 Hz, as used by Mecklenburg et al. (2011); they used a highpass cutoff of 39 Hz using an adaptive filter, which did not seem to isolate the OPs for our data, so the highpass was set to 100 Hz, as recommended by Marmor et al. (2009). Rangaswamy et al., (2006) also suggest limiting the lower cutoff to 100 Hz in order to be able to monitor changes in OPs (see Appendix for further discussion).

Equation 1 gives the transfer function of the Butterworth filter in MATLAB. The filter produces a lowpass filter of the nth order, with a normalized cutoff frequency. Row vectors b and a of size n+1 are returned as the coefficients of the filter, with descending power of z (www.mathworks.com). Further analysis and plots were generated with Microsoft Excel.

$$H(s) = \frac{B(s)}{A(s)} = \frac{b(1)s^n + b(2)s^{n-1} + \cdots + b(n+1)}{s^n + a(2)s^{n-1} + \cdots + a(n+1)} \qquad \textbf{Equation 1}$$

Where, H(s) is the transfer function; B(s) is the output and A(s) is the input of the transfer function.

The most easily discernible OP peaks were extracted from the strongest strength stimulus. An example of an ERG response to the strongest flash strength stimulus is presented in **Figure 4: A,** along with the extracted OPs from that response. When the

meERG and the extracted OPs are plotted in a zoomed in window of 70 ms, (**Figure 4: B**), a slight shift in phase is visible between the ERG and OPs waveforms. The International Society for Clinical Electrophysiology of Vision (ISCEV) guidelines report that depending on the type of filter that is used to extract the OPs, phase shift and ringing may occur in the extracted OP signal (Marmor et al., 2004).

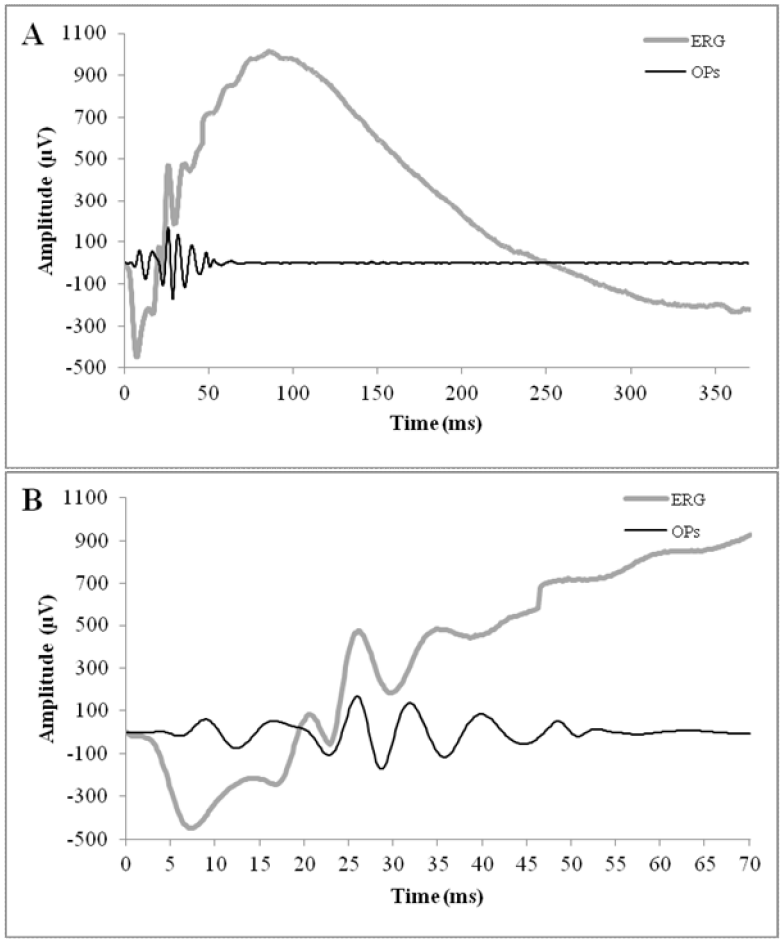

Figure 4 ERG signal from electrode A1, at the highest strength flash 159 sc cd s/m2, with the 4th order Butterworth filtered oscillatory potentials overlaid. (A) ERG and OPs in the ERG time range, 360 ms; (B) ERG and OPs zoomed in the OP time range, 70 ms.

b. Methods of Evaluating Amplitude: Two most common types of techniques for measuring OP amplitudes are the Peak-to-Trough method and the Caliper-Square method, explained below (Severns et al., 1994).

1. *Peak-to-Trough* ï Amplitude is determined by measuring the value between the preceding trough and the peak of the OP wavelet. The value of negative peak (trough) is determined and subtracted from the positive peak value. The resulting value is labeled as the total amplitude measured using the peak-to-trough method (**Figure 5**).

2. *Caliper-Square* ï Amplitude is determined by creating a line between the trough preceding a peak and the trough following the same peak. This line is indicated as the baseline for that particular peak. The amplitude is then measured, for the specific OP wavelet, from this baseline to the peak (**Figure 5**). The baselines may vary for all the peaks in one OP wavelet series.

3. *Sum of Peaks (SOP)* ï is determined by summing the amplitudes of all OP peaks in the series, which were determined either by the peak-to-trough method or the Caliper-Square method.

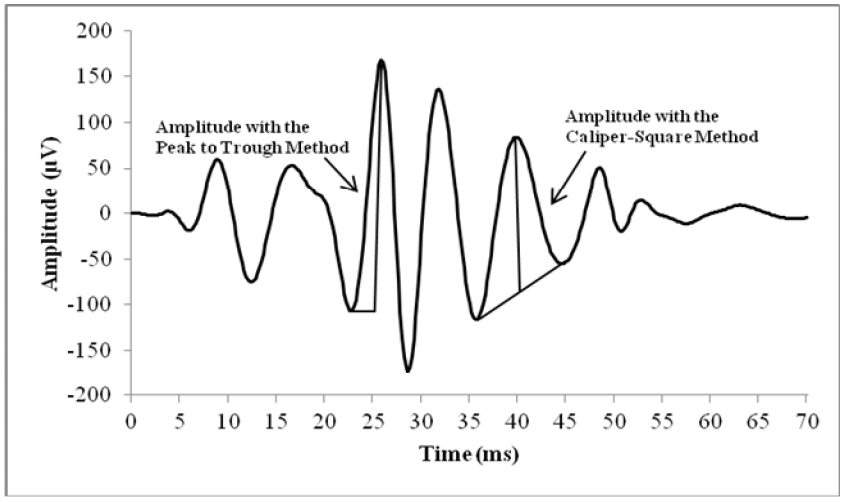

Figure 5 Schematic of amplitude measurement methods. The amplitude using the peak to trough method is determined by measuring the value from the preceding trough to the peak of the OP wavelet. The amplitude using the Caliper-Square method is determined by creating a line between two adjacent troughs and a perpendicular line from this baseline to the peak; the value of this perpendicular line is the amplitude of the peak.

Investigators have used a variety of approaches to analyze OPs. Since there are no definite guidelines to study OPs, the analysis method vary across the field. It has been commonly reported that the earliest OP peak is contaminated with the a-wave response and is usually not evaluated (van der Torren, et al., 1988; Asi et al., 1992; Bui et al., 2002; Moskowitz et al., 2005; Liu et al., 2006; Mecklenburg et al., 2011). Therefore, in this study the first visible peak was not included in the analysis. When the OPs are extracted from ERGs under variation in stimulus strength, the number of peaks varies and it can be hard to determine which peak is a true OP peak. As was seen in the reported data (e.g. Figure 6), the number of very prominent peaks for the strongest stimulus was six, and for the weakest, only two. In addition, there was an artifact seen for peak 6 and was also excluded from analysis. Therefore, for the purposes of this study, peak 1 and

peak 6 were excluded from analysis, and a total of 4 peaks were analyzed for all flash strengths. For the weaker stimuli two more, not so prominent peaks were analyzed, and threshold was set at 10 µV, which is much higher than previously reported threshold of 3 µV, reported for c57BL/6 rats at 100 cd s/m^2 (Mecklenburg et al., 2011). **Figure 6** gives a visual representation of the excluded peaks and analyzed peaks.

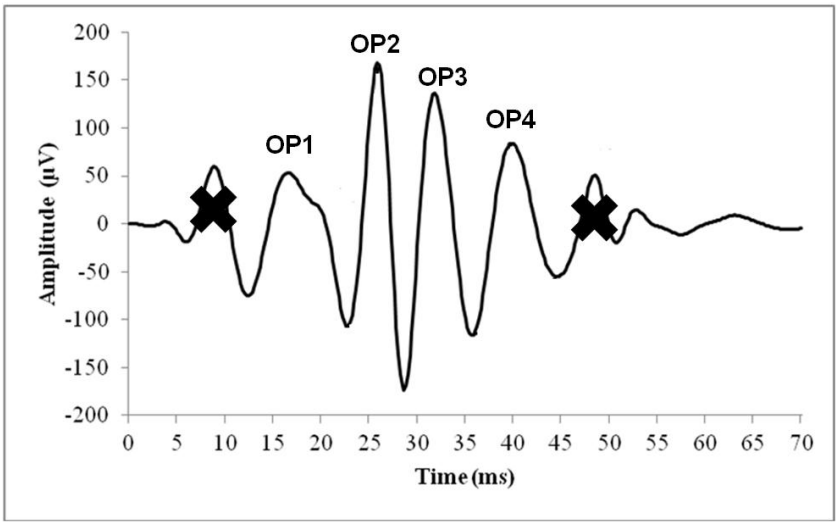

Figure 6 Visual representation of the OP peak analysis. The first peak occurring in the OP waveform was eliminated because it is known to be corrupted by the a-wave. The sixth peak occurring in the OP waveform was also excluded from analysis in this study, because there was an artifact seen in that peak for some responses. The OP analysis in this study, included OP1, OP2, OP3, and OP4. The sum of peak was therefore calculated as SOP = OP1 + OP2 + OP3 + OP4.

It has been reported that measuring OP amplitudes using either method should give nearly identical amplitudes; however, when the sum of peaks calculation is done using the peak-to-trough method, the estimate is smaller by approximately 5 µV, which is typically not significant for a clinical setting (Severns et al., 1994). Because of the ease in calculating and the small difference in determined amplitudes from either method, the peak-to-trough method was used in this analysis.

A meERG response at the highest flash strength for a 7 week old rat is depicted in **Figure 7**. The distribution of the ERG signal on the cornea is shown here in a ‘position plot’, which correlates to the spatial orientation of the 25 electrodes on the recording lens. The OPs extracted from the ERG response in **Figure 7**, using the 4th order Butterworth filter, is plotted in **Figure 8**.

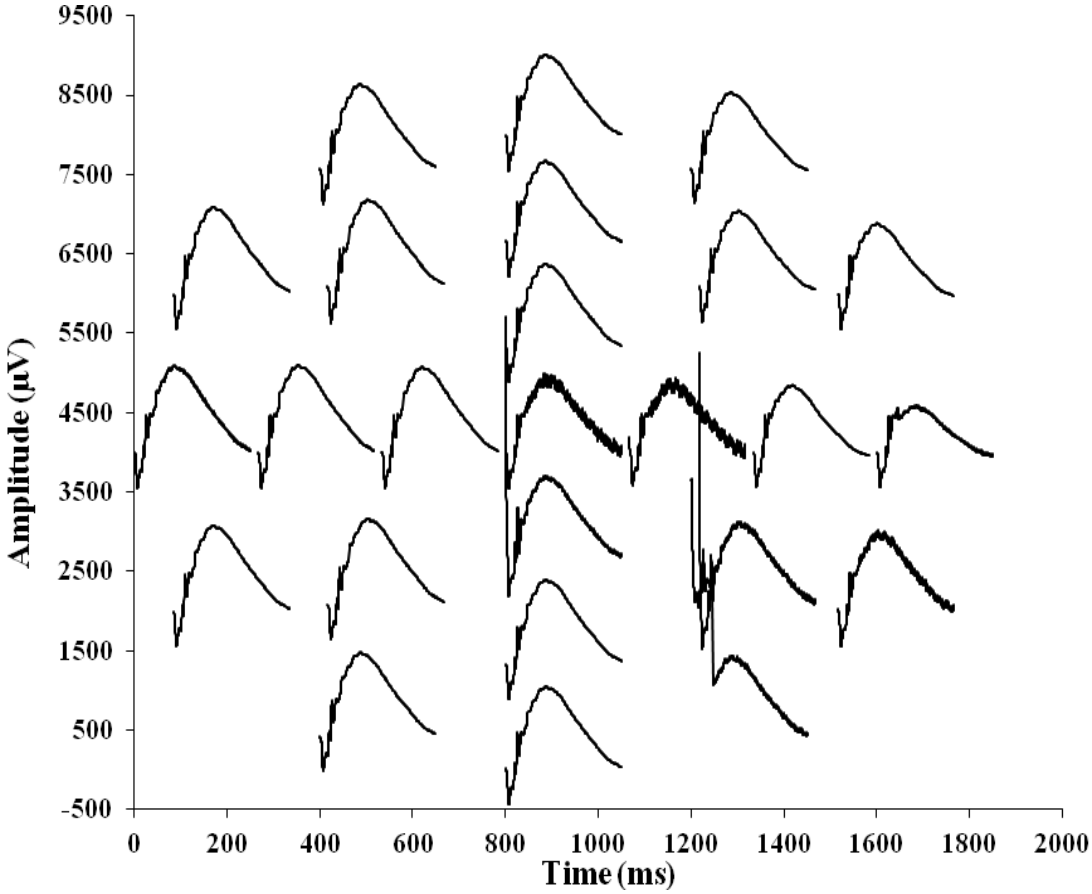

Figure 7 A meERG response. The meERG response is depicted in a ‘position plot’, for a 7 week old rat, at the strongest flash strength. The position plot correlates ERG signals to the 25 electrodes on the recording lens.

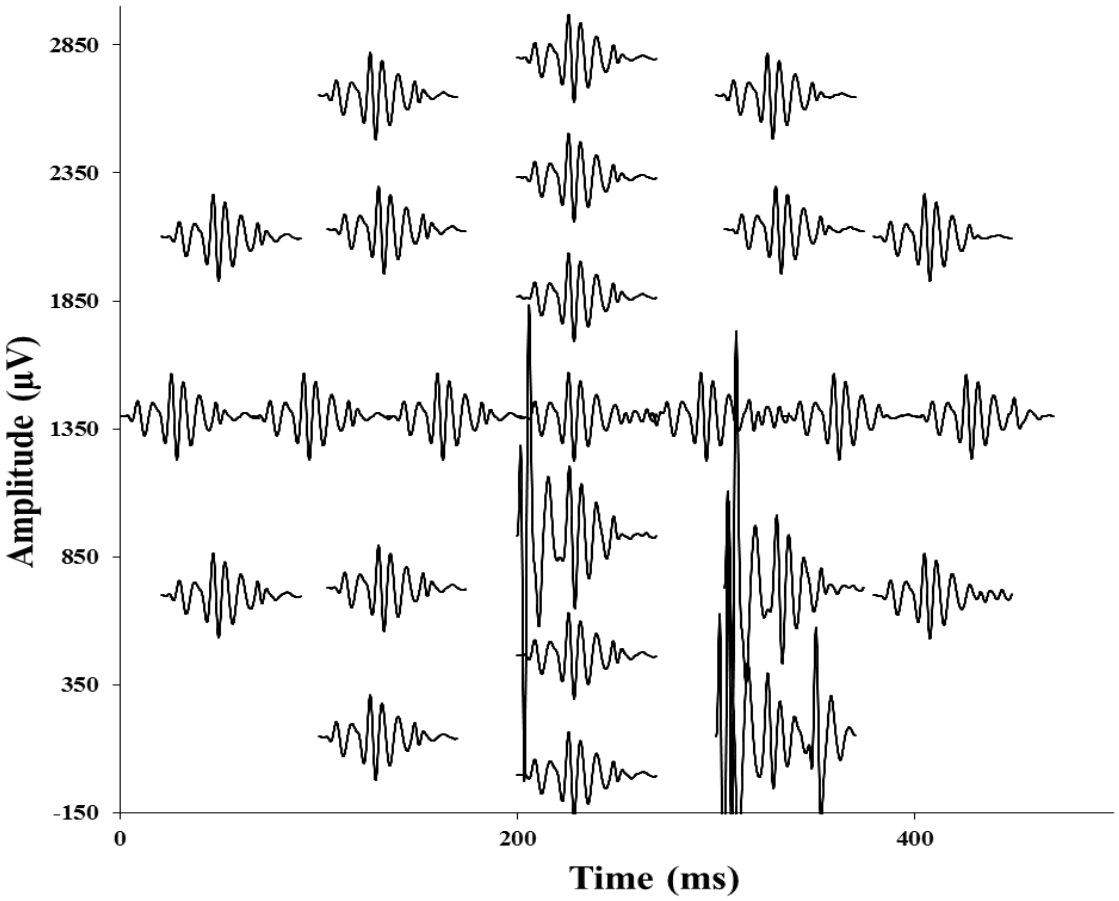

Figure 8 Extracted OPs from the meERG response. The OPs were extracted using the 4th order Butterworth filter and plotted in a position plot. The OPs are extracted from the ERG response in **Figure 7**.

Difference waveforms were determined by averaging the OP signal for all 25 electrodes, and then subtracting each single electrode OP from the average; as mentioned earlier, electrodes A6, B4, and C3 were not included in the average, due to the appearance of visually significant artifacts. A visual representation of this calculation is represented in **Figure 9.** The three excluded electrodes are represented as flat lines in the difference position plot.

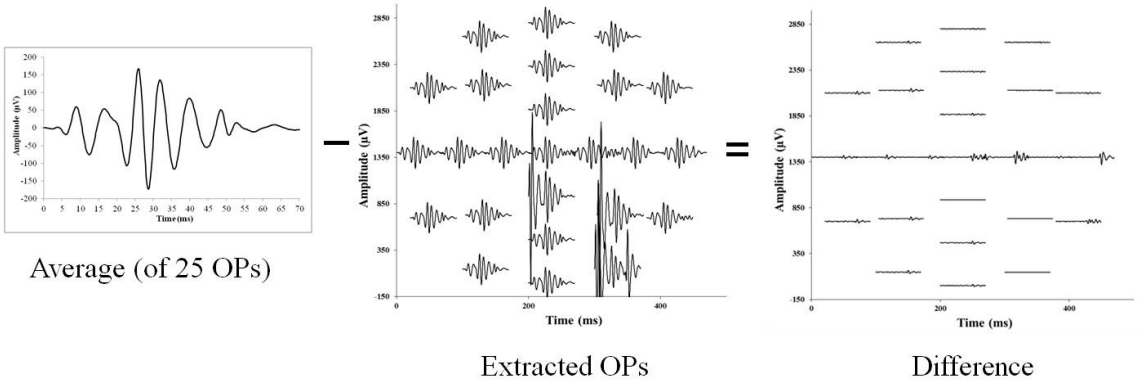

Figure 9 Difference calculation. The difference waveforms were calculated by averaging the OP signal of 25 electrodes, and then subtracting each electrode from that average. The resulting difference was almost flat for all electrodes. In the presented example, three of the electrodes in the response had an artifact; these electrodes were excluded from the average, and therefore the average was of 22 electrodes.

Representative plots for the raw meERG, extracted OPs and difference waveforms, showing spatial distribution of the responses are represented in **Figures 10-12**. These plots show responses obtained in one animal during one experiment at 7 weeks old. The distribution of the meERG signals, on the cornea, shown in ñposition plotsò, (**Figure 10: A-C**) correlates to the spatial orientation of the 25 electrodes on the

recording lens. The panels represent the meERG signals for three light stimuli, 0.01, 5.841, and 159 sc cd s/m^2. When comparing the three meERG position plots, it can be seen that the OPs become more visible with stronger stimuli; in addition, it can also be seen that the a-wave amplitude increases with the stronger stimuli.

The OPs, which were extracted using a 4^{th} order Butterworth filter (passband: 100 Hz - 300 Hz), for each stimulus, are represented in **Figure 11: A-C**. Comparing the OP position plots, it can be seen that the amplitudes and the number of OPs that appear are greater as the stimulus strength increases. It can also be seen that the appearance of the OPs with the weakest stimulus is delayed. In this experiment, a significant amount of artifact is visible for electrodes A6, B4 and C3, for all flash stimuli; these electrodes will not be used for further analysis of OPs and difference plots. Similarly, channels with high noise or large artifacts were not included in the analysis of other data sets. The difference waveforms for extracted OPs, as determined in **Figure 9**, are represented in **Figure 12: A-C**.

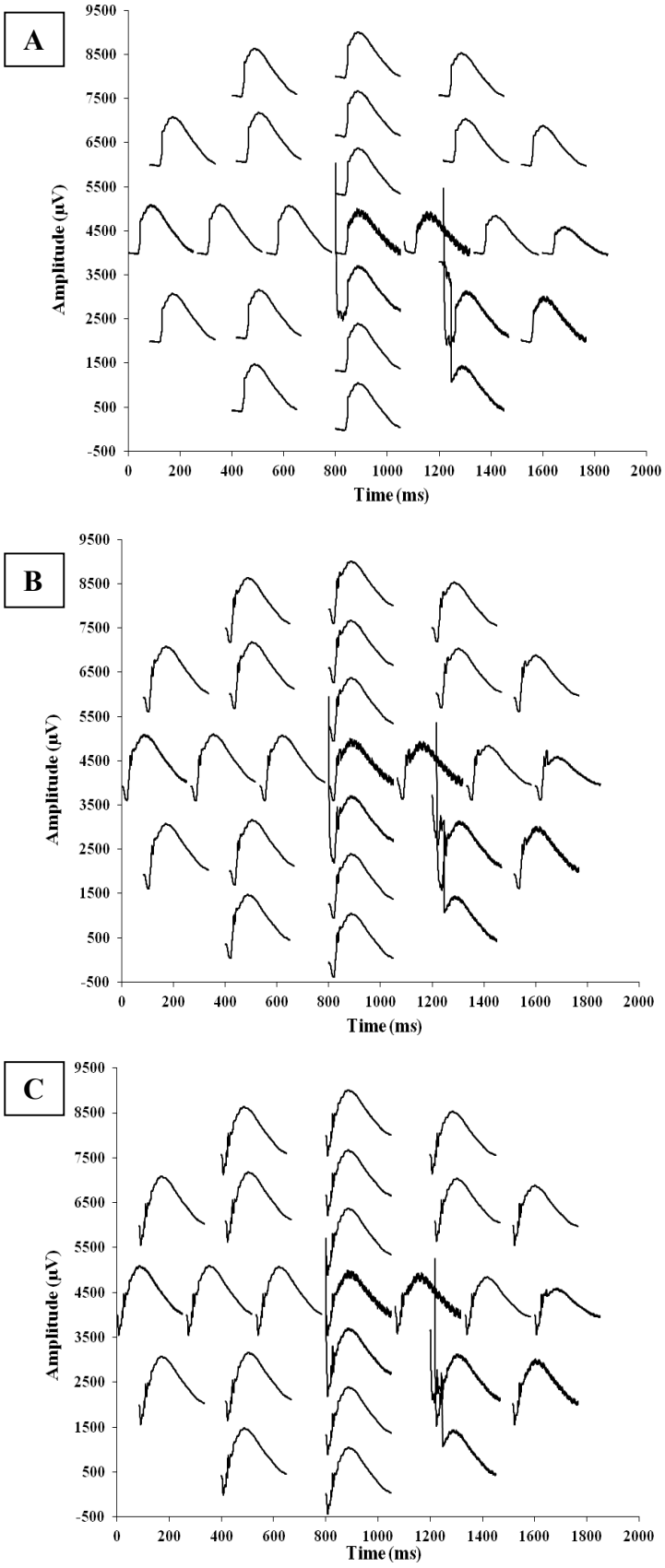

Figure 10 Position plots of the raw meERG, from one rat. Panels A, B and C correspond to stimulus strengths, 0.01, 5.841, and 159 sc cd s/m^2, respectively. Waveforms begin at t = 0, time of stimulus.

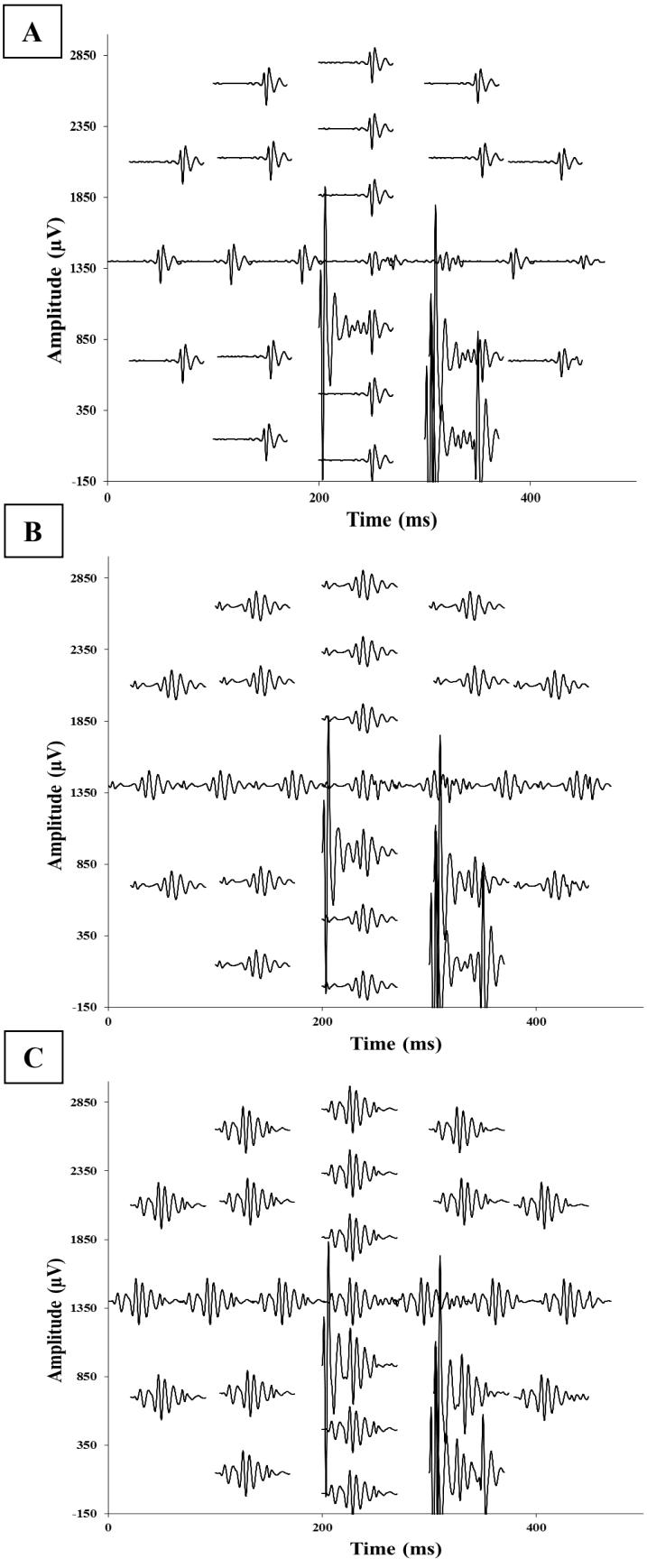

Figure 11 Position plots of the extracted oscillatory potentials isolated from waveforms shown in Figure 5. Panels A, B and C correspond to stimulus strengths, 0.01, 5.841, and 159 sc cd s/m^2, respectively. Waveforms begin at t = 0, time of stimulus. Artifact was seen in electrodes A6, B4, and C3, which were excluded from analysis.

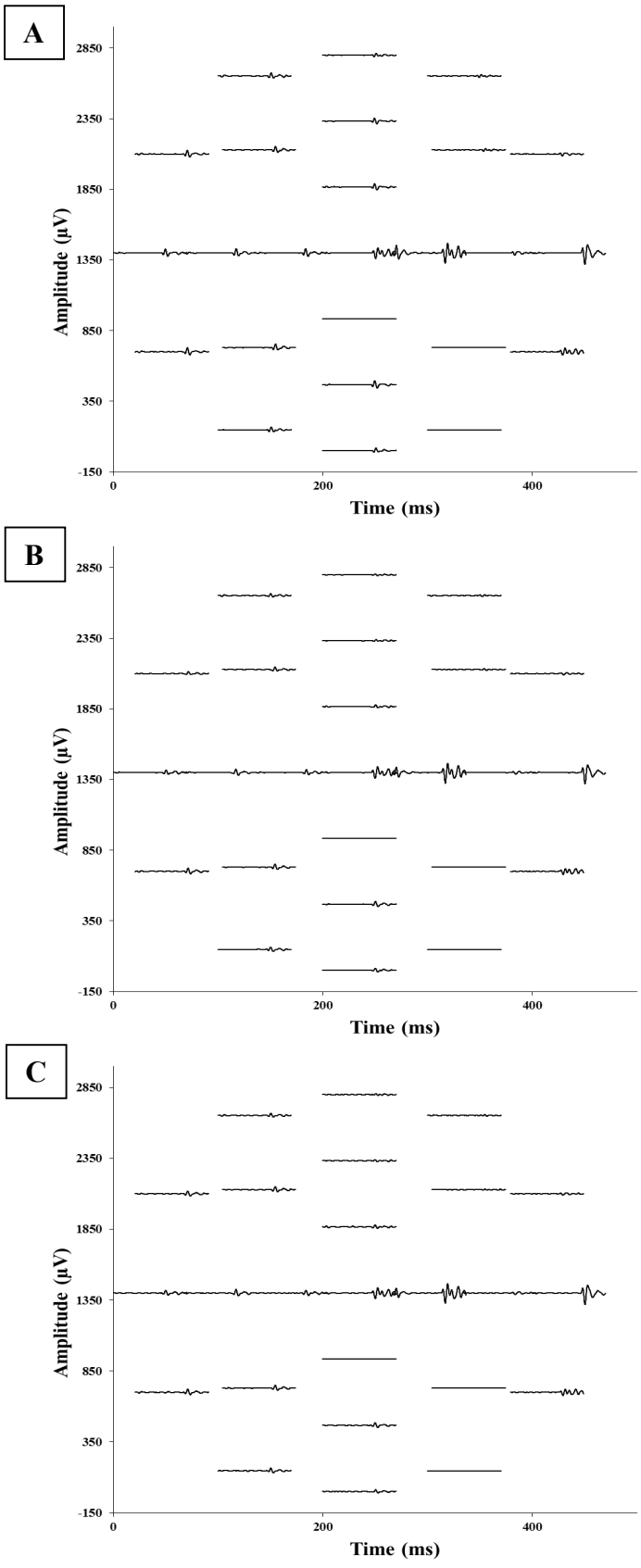

Figure 12 Position plots of the difference waveform. Differences were obtained from OP waveforms shown in Figure 6, as explained in the text. Panels A, B and C correspond to stimulus strengths 0.01, 5.841, and 159 sc cd s/m^2, respectively. Waveforms begin at t = 0, time of stimulus.

Figure 13 shows the relationship between the extracted OPs and stimulus strength. A delay in the appearance of OPs can be seen with decreasing strength. A decrease in amplitudes is also seen between the low strength stimulus responses, 0.01 sc cd s/m^2, and 5.841 sc cd s/m^2 compared to the highest stimulus strength, 159 sc cd s/m^2. The peak labelled as OP1, for each OP response, is indicated by an arrow.

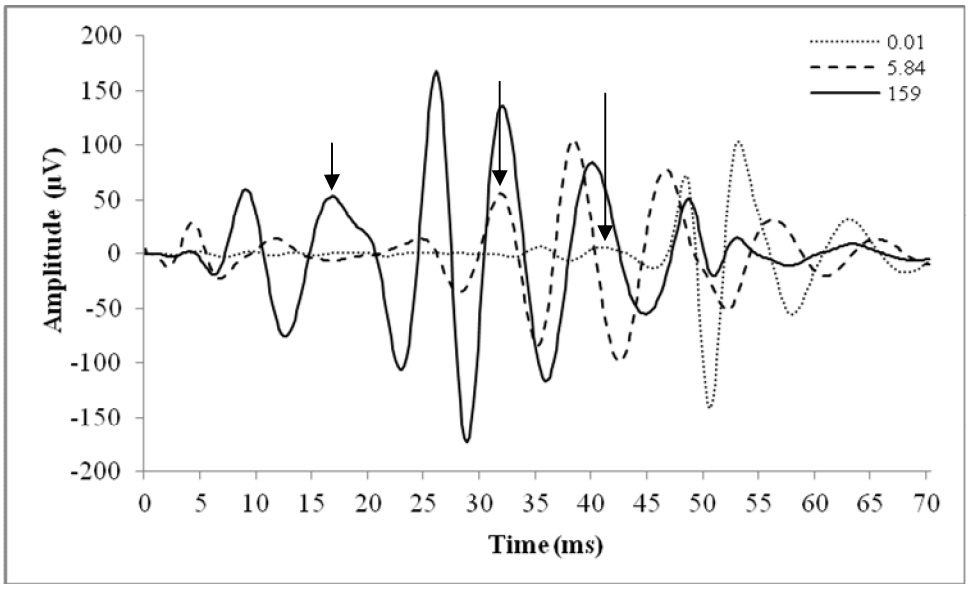

Figure 13 Extracted OP for three light stimuli, 0.01 sc cd s/m^2 (dotted line), 5.841 sc cd s/m^2 (dashed line), and 159 sc cd s/m^2 (filled line). First peak for each response is indicated by an arrow.

As explained previously, the difference plots were produced by taking the average of OP signal from all electrodes and then subtracting the OP signal of each electrode from that average. Difference plots were generated to visualize the minor variations between the OPs extracted from the 25 electrodes for each recording. If the OP signal of an electrode was close to the average of all the electrodes, the difference approximates a flat line, (**Figure 14: A**). However, if the OP signal of an electrode is different than the average of all electrodes, the difference is a waveform with peaks, (**Figure 14: B and C**); this is most visible where the peak is steep and its amplitude is large, as seen in the third peak in **Figure 14: B and C**. Plotting the difference waveforms for the individual electrodes on a second y-axis, (**Figure 15: A-C**), makes it easier to visualize these variations.

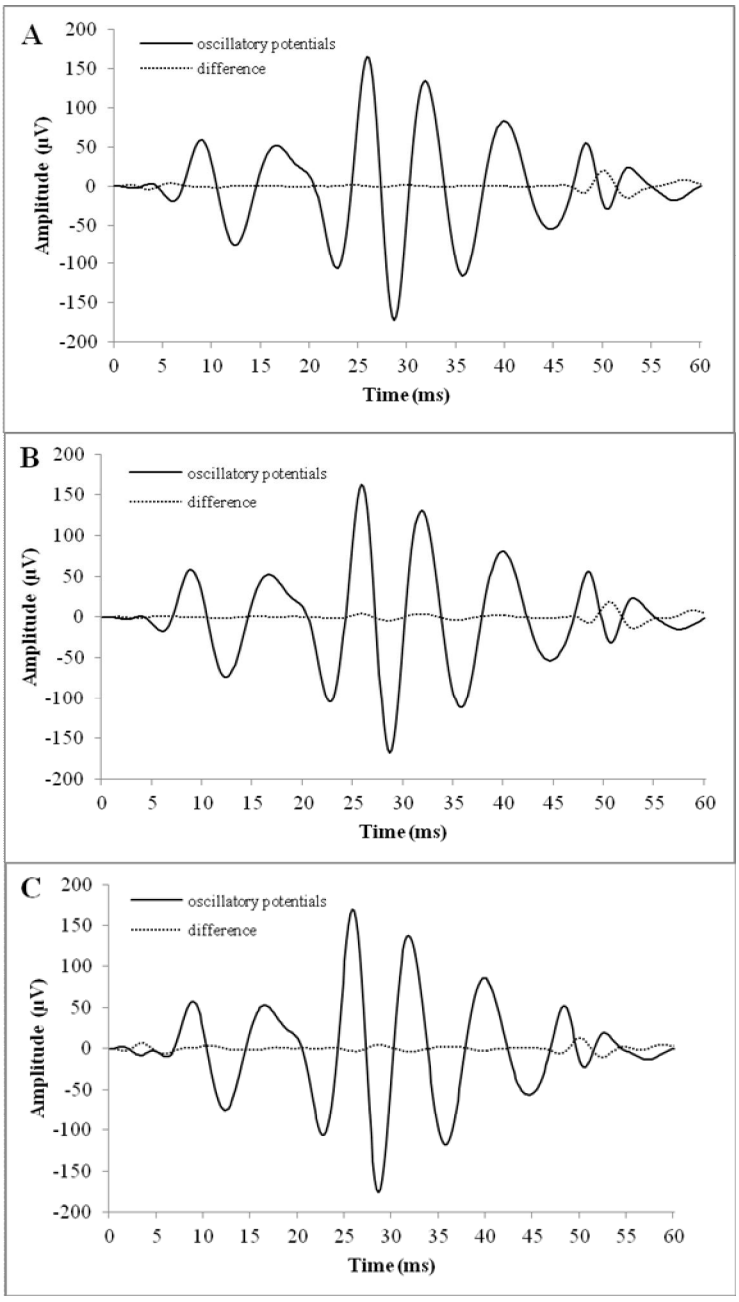

Figure 14 Extracted OPs with difference waveform. (A) OP signal (of electrode A11) where the average of all electrodes, in the meERG, is approximately equal to the signal (of electrode A11). The difference is almost flat; (B) OP signal (of electrode A8) where the signal (of electrode A8) is less than the average of all electrodes in the meERG. The difference is slightly above the baseline for each peak; (C) OP signal (of electrode C1), where the average of all electrodes in the meERG is less than the signal (of electrode C1). The difference is slightly below the baseline at each peak.

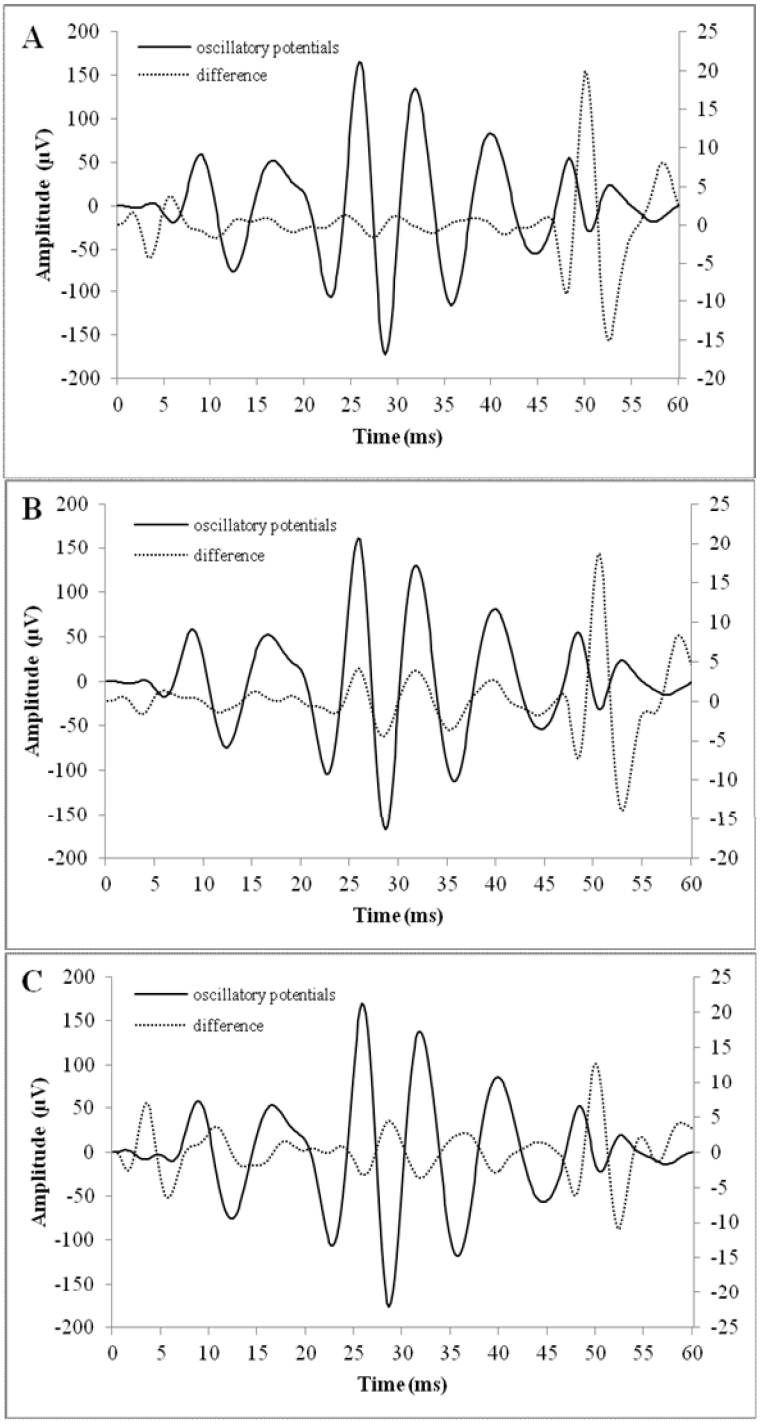

Figure 15 Extracted OPs with difference waveform (on secondary axis). (A) OP signal (of electrode A11) where the average of all electrodes, in the meERG, is approximately equal to the signal (of electrode A11). The difference is almost flat; (B) OP signal (of electrode A8) where the signal (of electrode A8) is less than the average of all electrodes in the meERG. The difference is slightly above the baseline for each peak; (C) OP signal (of electrode C1), where the average of all electrodes in the meERG is less than the signal (of electrode C1). The difference is slightly below the baseline at each peak.

IV. Results

A. To the authorôs knowledge, this is the first description of the variation of OP amplitude with position across the cornea, enabled by the novel meERG recording approach. The overall goal of this work is to characterize these spatial differences in normally-sighted rats, to begin the formation of a normative data base for this unique type of measurement. In this way, the normal range can be defined, and used as a reference for noting differences from normal associated with experimental or clinical variables, such as disease state. The initial goal was to evaluate the variation in OP amplitude as a function of position across the cornea; therefore, ***Specific Aim 1*** *was to analyze variation of OP amplitudes across electrode positions in individual meERG responses*. The variance at a single flash strength will be characterized in nine animals.

Variance of amplitudes across electrodes was analyzed at the highest flash strength, 159 sc cd s/m^2, to characterize the difference between each electrode in a single recording. The variance was normalized by dividing the statistical variance of amplitudes across all 25 electrodes by the average of the amplitudes of the 25 electrodes (Equation 2). **Figure 16** depicts the normalized variance of sum of peaks of OPs for all 9 rats at 6 and 7 weeks of age (18 data sets). The variance across electrode positions was typically 10-30% of the mean amplitude. The unusually high variance calculated for some of the experiments was most likely due to procedural anomalies, and do not reflect the variance of the meERG potentials at the cornea.

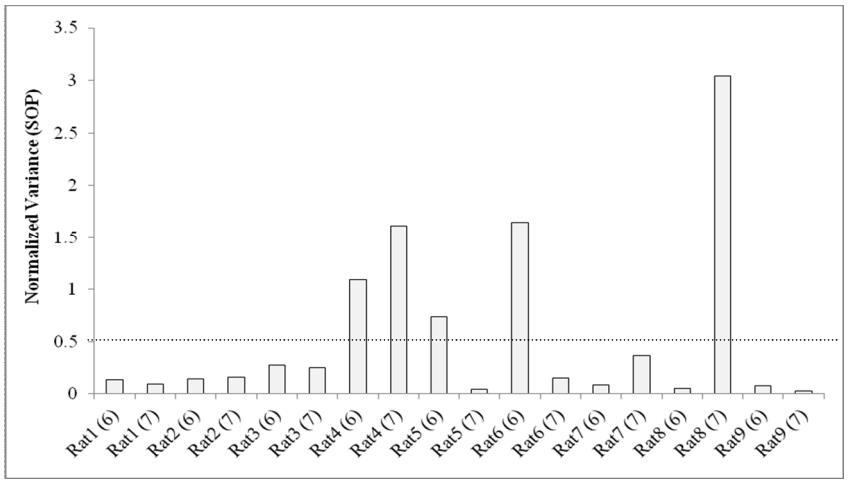

Figure 16 Normalized variance of Sum of Peaks of OPs for nine rats at 6 and 7 weeks of age. The normalized variance was seen to be typically 10-30% of the mean amplitude. Dotted line at 50% variance is shown for visual reference.

The same SOP variances from **Figure 16** are plotted in **Figure 17**, along with the normalized variances of the a-wave and the b-wave. The dotted line at 50% variance is marked for visual reference. No relative trend was seen in the variance values; however, in 14 out of the 18 experiments, a-wave had a higher variance than OPs and in 15 out of the 18 experiments, b-wave had a higher variance than OPs. This implies the different spatial distributions of the cells that give rise to the OP, a-wave and b-wave components of the ERG. The variance data used in **Figure 16** and **Figure 17**, is given in **Table 1**.

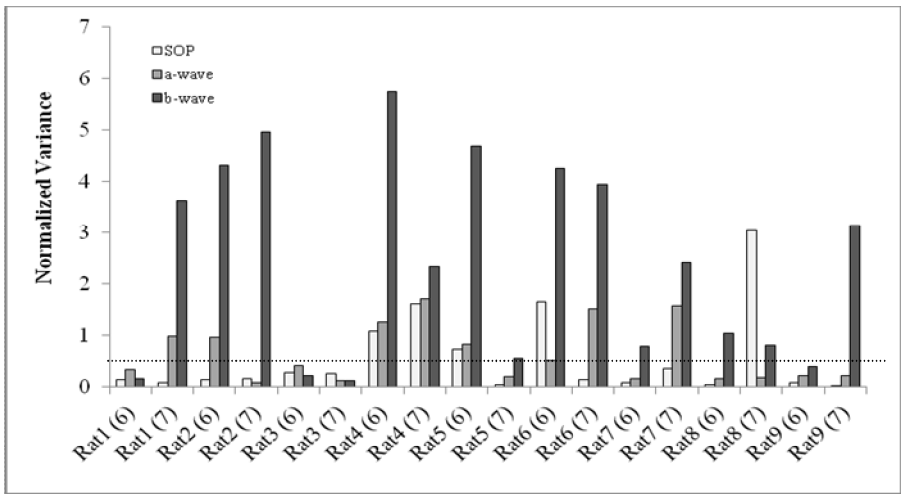

Figure 17 Normalized variance of sum of peaks of OPs, the a-wave and the b-wave, for 9 rats at 6 and 7 weeks of age. All responses evoked with 159 sc cd s/m^2 stimulus. Dotted line at 50% variance is shown for visual reference.

Table 1. Normalized variance values plotted in Figure 16 and 17. The normalized variance values of the sum of peaks of OPs, a-wave and b-wave are presented here, for 9 rats at 6 and 7 weeks of age.

Rat Number	Experiment Number	Normalized Variance of SOP	Normalized Variance of a-wave	Normalized Variance of b-wave
Rat1 (6)	1	0.1364	0.3430	0.1624
Rat1 (7)	2	0.0922	0.9933	3.6418
Rat2 (6)	3	0.1414	0.9697	4.3203
Rat2 (7)	4	0.1622	0.0869	4.9647
Rat3 (6)	5	0.2776	0.4248	0.2325
Rat3 (7)	6	0.2530	0.1331	0.1165
Rat4 (6)	7	1.0877	1.2663	5.7456
Rat4 (7)	8	1.6111	1.7152	2.3491
Rat5 (6)	9	0.7334	0.8316	4.7004
Rat5 (7)	10	0.0428	0.2113	0.5551
Rat6 (6)	11	1.6461	0.5086	4.2564
Rat6 (7)	12	0.1458	1.5089	3.9409
Rat7 (6)	13	0.0835	0.1609	0.7849
Rat7 (7)	14	0.3648	1.5764	2.4201
Rat8 (6)	15	0.0476	0.1655	1.0495
Rat8 (7)	16	3.0394	0.1858	0.8111
Rat9 (6)	17	0.0775	0.2189	0.3918
Rat9 (7)	18	0.0230	0.2318	3.1379

Distribution of ratio of the sum of peak amplitude in the periphery to the center is depicted in **Figure 18**, for nine rats at 6 weeks of age **(Figure 18: A)** and 7 weeks of age **(Figure 18: B)**. The frequency of the ratio characterizes the relative difference of spatial distribution within a recording. Many more data sets are being collected to be added to the normative distribution. The symmetry of the distribution ratio is expected to change in a disease state.

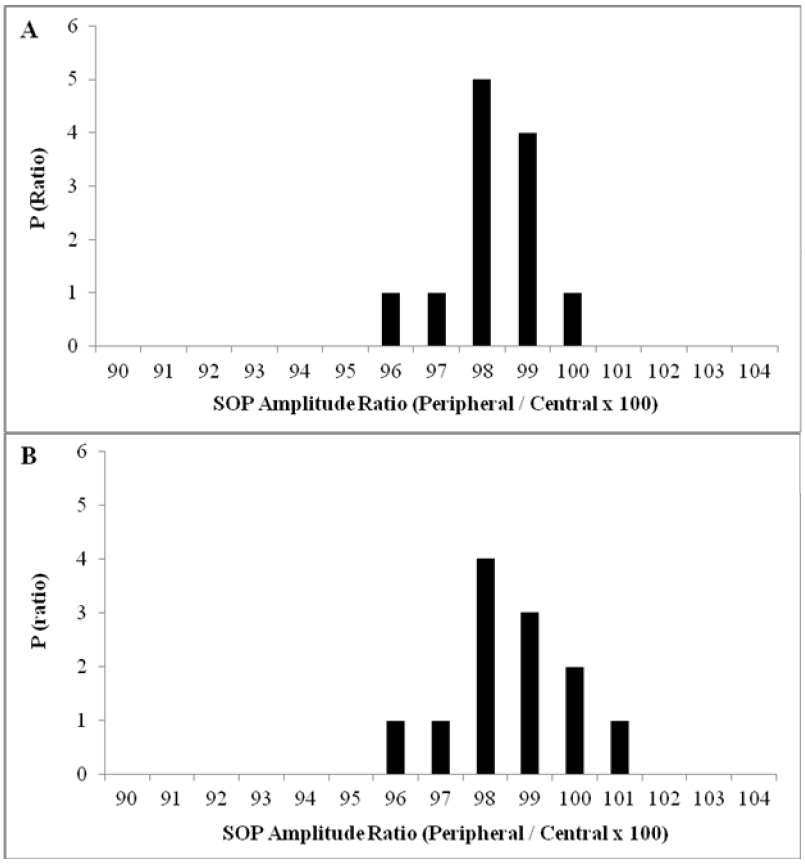

Figure 18 Distribution ratio. Frequency of distribution ratio is represented for nine rats at 6 weeks of age (A) and 7 weeks of age (B). More data will be added to this normative distribution. It is expected that disease states would modify the symmetry of this distribution.

B. The eye can be considered to be approximately radially symmetric about the visual axis (the line extending from the corneal pole to the back of the eye). For this reason, any spatial variation of corneal potentials would be expected to also be radially symmetric about the corneal pole. Based on this line of thought, the meERG potentials were grouped by ring (A, B, C, M), and these ring-averages amplitudes were compared. This is similar to the ring averaging employed when analyzing multi-focal ERG amplitudes, and has the advantage of increasing signal to noise ratio when looking for differences in amplitude as a function of radial eccentricity. Therefore, ***Specific Aim 2*** *was to analyze variation of OP amplitudes as a function of radial eccentricity on the cornea.* This was done in three animals, and for responses recorded following the highest flash strength used, 159 sc cd s/m^2.

The electrodes are grouped by rings because radial symmetry is assumed. This grouping should allow increased SNR, similar to the ring average approach used in mfERG analysis. **Figure 19** shows averages of individual OP peaks, OP1 - OP4, for each ring of electrodes, A ring, B ring, C ring and the middle M electrode. These are ring averages for one animal (rat 4) at 7 weeks of age. All pairs had a p-value > 0.05 (ANOVA), implying that the rings did not show variability. Please also note that there is no standard deviation for the middle electrode. The same analysis was done for two other animals, and the trend was the same. **Figure 20: A-C** is representation of peaks, OP1 - OP4, at 159 sc cd s/m^2 stimulus strength, for three different rats. For all three rats, OP3 has the highest amplitude for the A ring, B ring, C ring and the middle electrode, and OP1 was seen to have the lowest amplitude for all three rings for the three rats. OP peak 3 for rat 6 was the only peak which had a p-value < 0.05 (ANOVA).

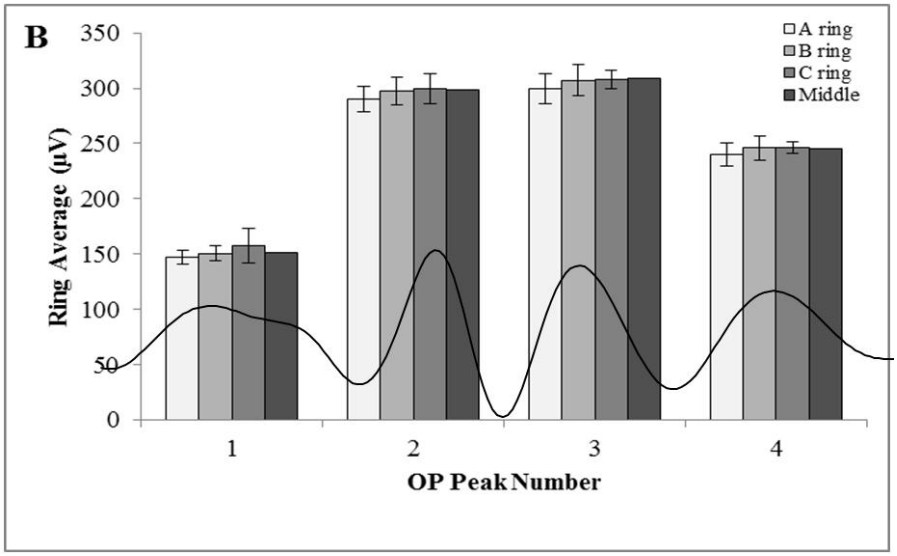

Figure 19 Ring averages of individual OP peaks for one animal. Ring averages at individual peaks for one animal (rat 4), at 7 weeks of age is represented here, along with an overlay of the OP waveform for visualization purposes. Average of amplitudes in A ring (white), B ring (light grey), and C ring (dark grey); middle electrode (black) did not have an average.

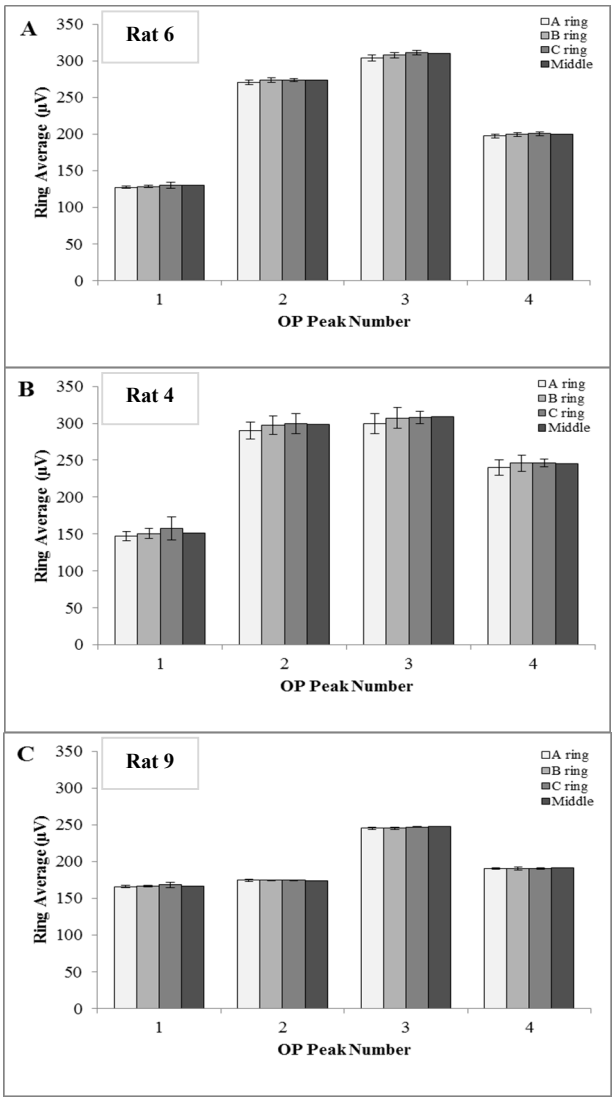

Figure 20 Ring averages of individual OP peaks for three animals. Average of amplitudes in A ring, B ring, and C ring; middle electrode did not have an average. Panels A-C are ring averages from 3 different animals at 7 weeks of age; A: Rat 6, B: Rat 4, C: Rat 9.

Table 2. Table of p-values derived using ANOVA across rings for each peak in each rat, in Figure 20.

	OP Peak 1	OP Peak 2	OP Peak 3	OP Peak 4
Rat 6	0.089	0.071	0.017	0.11
Rat 4	0.18	0.37	0.46	0.43
Rat 9	0.099	0.98	0.19	0.83

C. An important purpose of this study was to collect normative data for the novel meERG technique in Long-Evans rat. It is expected that when comparing normal sighted rats, the OPs between one animal to the next would be nearly identical. However, there may still be sources of variance which cannot be controlled or accounted for. By repeating the same protocol in animals that are as close to being identical, this variance can be determined. Characterizing how much the normal response varies within a general population, it would allow identification of óabnormalô response, which would be outside the range of the normal response. Therefore, ***Specific Aim 3*** *was to analyze variation of OP amplitudes between animals*. Mean amplitudes of sum of peaks, at each degree of corneal eccentricity (ñringsò), will be evaluated.

Figure 21 represents the average of ring SOPs for nine rats at 6 weeks of age. When comparing each ring (A-C), among the nine rats, the rings were significantly different between the rats (Ring A: p-value < 0.0001, Ring B: p-value < 0.0001, Ring C: p-value < 0.0001; ANOVA). The p-value for the middle electrode cannot be calculated because there is only one value for each animal. Because the meERG approach is based on spatial differences within an animal, as examined in specific aim 1 and specific aim 2, the difference between animals is not a weakness of the overall approach.

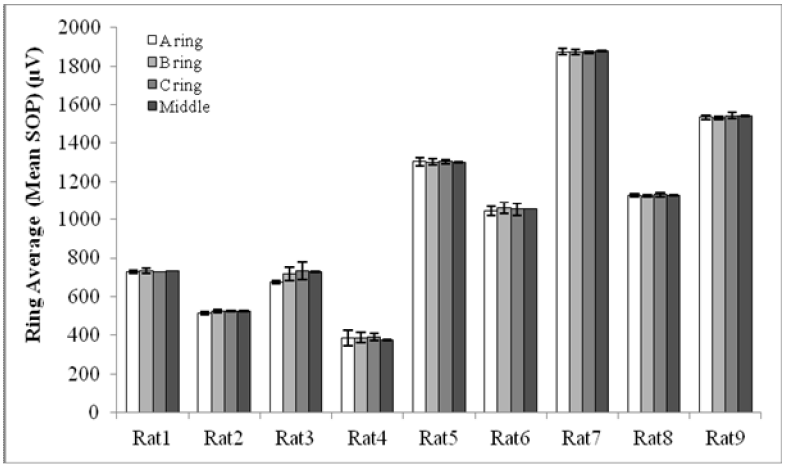

Figure 21 Average of ring SOPs. Average of SOPs for A ring, B ring, C ring electrodes and middle electrode for 9 rats, at 6 weeks are shown here. P-values derived using ANOVA, of SOP values across 9 rats of 6 weeks, for each ring. Please note that p-value cannot be derived for Middle electrode. Ring A: p-value < 0.0001, Ring B: p-value < 0.0001, Ring C: p-value < 0.0001.

D. Since the approach of the meERG is to measure variability within an animal, doing a repeated measure would allow characterizing how much the OPs vary in the same subject from one test to the next. It allows creating a baseline measurement and measure response due to changing conditions, such as response to a treatment or severity of a disease state. Since there are likely changes beyond control, this would allow understanding of how much the repeated measures vary, and get a measure of œexpected varianceô to be able to understand how much of a change in results is meaningful. Therefore, ***Specific Aim 4*** *was to analyze variation of OP amplitudes for repeated measures (one week apart) on the same animals*.

The OP amplitudes were compared at 6 and 7 weeks of age. The average SOPs for each ring of electrodes, (A-C), and the middle electrode are represented in **Figure 22**. The data in **Figure 22** was obtained for nine different rats at 6 weeks and 7 weeks of age at the highest strength stimuli, 159 sc cd s/m^2. The amplitudes are plotted by rings. The average amplitudes of the A ring, B ring, C ring, and the middle electrode, for each experiment, was seen to be approximately the same throughout all experiments. In addition, six out of the nine rats had a decrease in average SOP amplitudes from 6 weeks of age to 7 weeks of age. The lowest calculated SOPs for all experiments was about 390 µV and the highest calculated SOPs was about 1870 µV. To make it easier to visualize, the data in **Figure 22** is broken down by rings in **Figure 23: (A-D)**, and pair-wise t-test analysis is shown for all rings. The p-values with t-test cannot be calculated for the middle electrode SOPs, because there is one value for middle SOP in each experiment. The animals had a statistically significant difference in amplitude between 6 and 7 weeks

of age, (p-value < 0.05, studentôs t-test, power > 80%, except Ring B for rat 4 power: 72.1%. Ring C for Rat4: p-value > 0.05 (studentôs t-test, power: 53.5%).

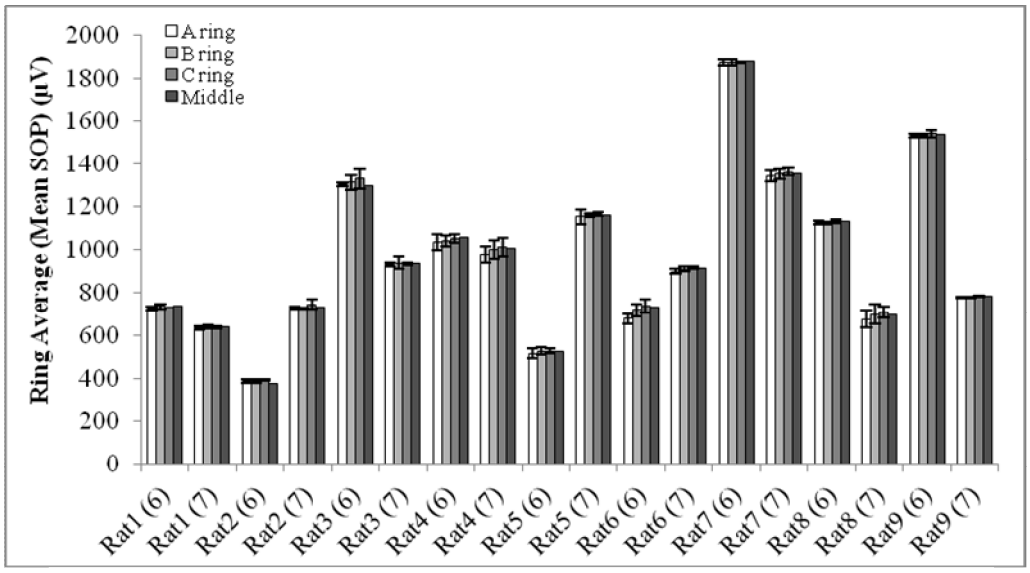

Figure 22 Average of ring SOPs for all experiments. Average of SOPs for A ring, B ring, C ring electrodes and middle electrode for 9 rats, at 6 and 7 weeks are shown here.

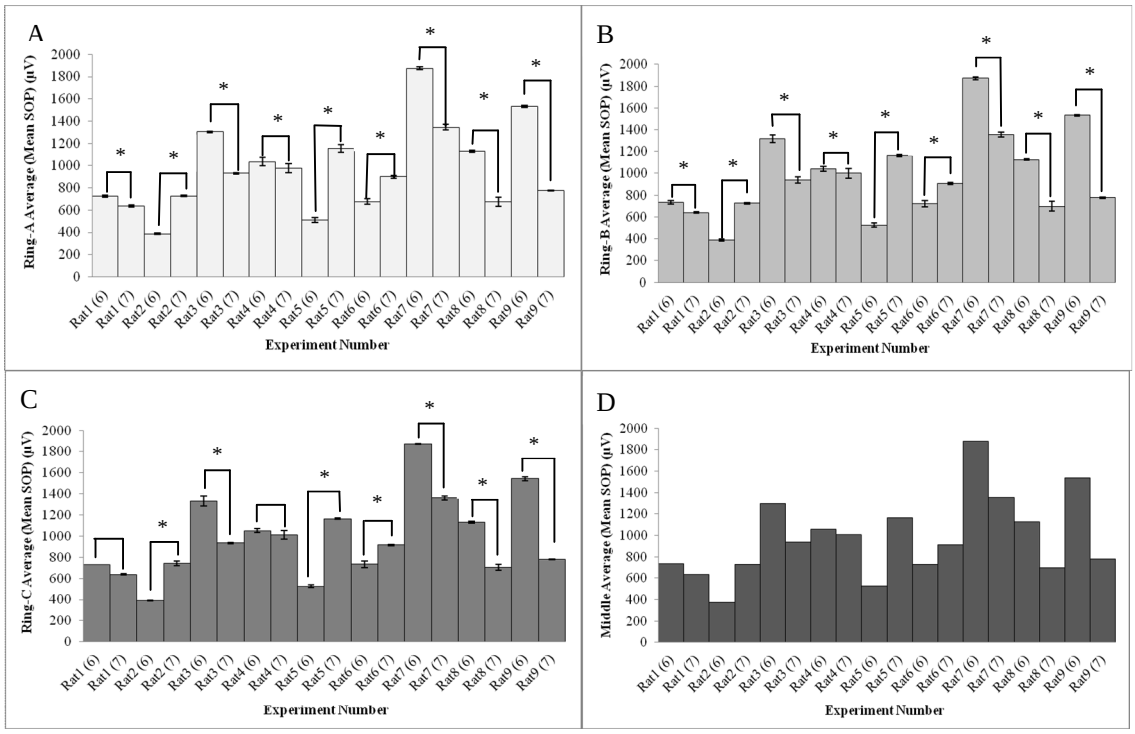

Figure 23 Average SOPs for all experiments, by rings. Average of SOPs for A ring, B ring, C ring electrodes and middle electrode for 9 rats, at 6 and 7 weeks are shown in panels A-D.

Figure 24 represents the average amplitudes of OPs for all electrodes for nine rats at 6 and 7 weeks of age. Similar to the data seen in **Figure 22**, the six of the nine rats showed a decrease in average amplitude of OP from 6 weeks to 7 weeks of age. The p-values obtained using t-test for the nine pairs of experiments are also represented. All pairs had a p-value < .05 (statistical power: 100%).

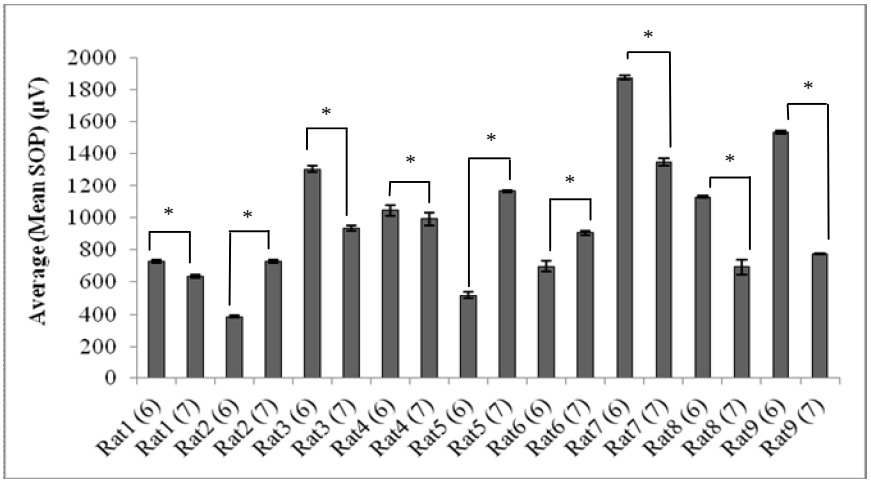

Figure 24 Average SOPs for all experiments. Average of SOPs of all electrodes for 9 rats, at 6 and 7 weeks are shown here. Pair wise comparison between the groups of 6 and 7 weeks, for each rat resulted in p values < 0.05.

Variation of latencies of OP amplitudes was evaluated as a function of stimulus strength. The effect of the strength of the light stimulus on the latency of the OPs was studied. OP signals extracted from meERG signals recorded at stimulus strengths, 0.01, 5.841, 19.98, 30.4, 73.4, 116.4, and 159 sc cd s/m^2 were evaluated. The latency was calculated as the sum of the total time to peak (TTP) of the four OP peaks; the TTP for 25 electrodes was averaged and is a represented in **Figure 25,** against the log of the stimulus strengths. The latency of the OPs is linear with respect to the log of the stimulus strength, with OPs having a higher implicit time at low stimulus strengths and shorter implicit time at higher stimulus strength.

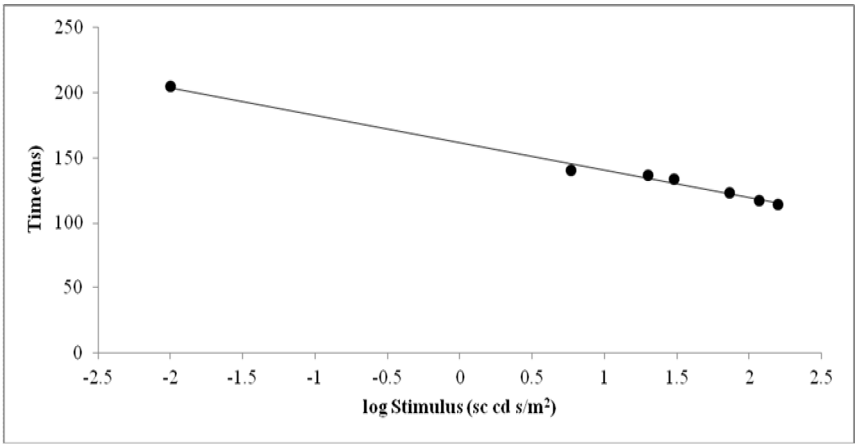

Figure 25 Average of the sum of peak latencies vs. log of stimulus strength. The sum of the peaks latencies of all electrodes were averaged for the stimulus strengths.

A different representation of the effect of stimulus strengths on the total time to peak of the OPs is represented in **Figure 26**. The average of all electrodesô implicit time for each OP peak is graphed against log stimulus strength. It can be seen that the implicit time to peak of each OP peak is inversely related to the log of stimulus strength, with OP1 requiring the shortest amount of time to peak and OP4 requiring the longest time to peak.

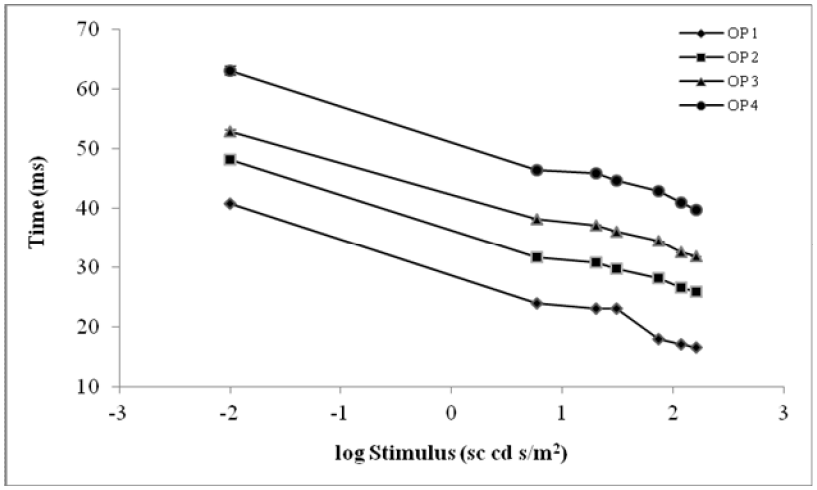

Figure 26 Implicit times of OP1, OP2, OP3, and OP4 vs. log strength. The average of implicit time for each OP peak from all 25 electrodes is represented here, against the log of the stimulus strength.

Stimulus Response Function was determined, by evaluating dependence of OP amplitude on stimulus strength. The effect of the strength of the light stimulus was studied. OP signals extracted from meERG signals recorded at, 0.01, 5.841, 19.98, 30.4, 73.4, 116.4, and 159 sc cd s/m^2 were evaluated. The SOPs for all 25 electrodes were averaged and are represented in **Figure 27**, versus the log of the stimulus intensities. The SOP amplitudes increase with higher stimulus strength, and the two lowest strength stimuli have almost the same amplitude.

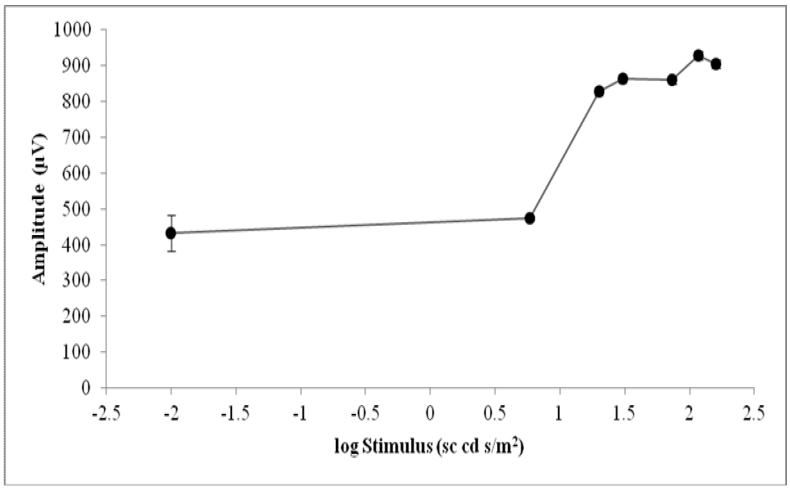

Figure 27 Average SOPs vs. log of stimulus strength. The SOPs of all electrodes that were averaged, for the stimulus intensities, are represented here.

A different representation of the effect of stimulus strengths is represented in **Figure 28**. The average of all electrodes for each OP peak is graphed against log stimulus strength. The amplitude of OP1 and OP2 for the smallest two light stimuli is about the same. For the higher intensities for OP1, there is a linear relationship between the OP amplitudes and the log flash strengths. The relationship between the amplitudes of OP4 at higher strength stimuli is nearly horizontal; the OP4 amplitude at intensities 19.98 sc cd s/m^2 is almost the same. There is a significant increase in amplitude of OP2 and OP3 with an increase from 5.841 sc cd s/m^2 to 19.98 sc cd s/m^2.

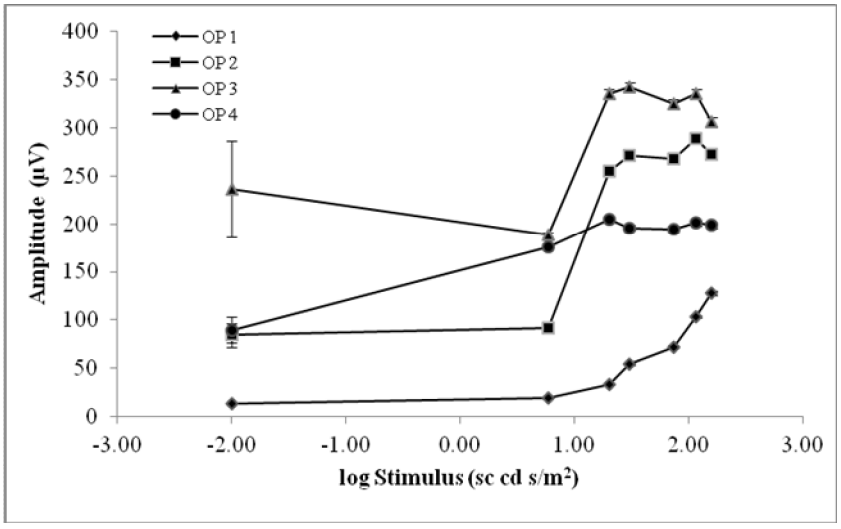

Figure 28 OP1, OP2, OP3, and OP4 vs. log stimulus strength. The average of amplitude for each OP peak from all 25 electrodes is represented here, against the log of the stimulus strengths.

V. Discussion

In the present study, the multi-electrode ERG (meERG) was used to acquire normative data on the spatial orientation of the oscillatory potentials (OPs), in a rat model. It was found that the average sum of peaks (SOP) amplitude increased with increase in stimulus intensities, and SOP amplitudes at 0.01 and 5.841 sc cd s/m^2 are nearly the same. When analyzing individual OP peaks, OP1 amplitude increased with increasing stimulus strength, and the amplitude of OP4 did, at higher strengths, did not vary much, though the amplitude at 0.01 sc cd s/m^2 was much lower than at other strengths. Average amplitude of OP2 and OP3 also had a large increase from 5.841 to 19.98 sc cd s/m^2, but no major variation was seen at higher intensities. In addition to the attenuation of OP amplitude, the appearance of first visible peaks was also prolonged in weaker stimuli, similar to previous findings (Liu et al., 2006).

When comparing the average of OP response for each ring of electrodes, it was seen that OP3 has the highest amplitude for all rings, A ring, B ring, C ring and the middle electrode, followed by OP2, OP4 and OP1. This is similar to previous findings that the higher amplitude peaks are OP3 and OP2, and OP1 and OP4 have lower amplitudes (Hancock et al., 2008).

Additionally, when the average SOP of the 9 rats at 6 and 7 weeks were compared in this study, there was great variability in the amplitude of OPs between the rats; however, the amplitude of rings for each animal did not significantly vary.

Even though the cellular origin of the OPs is still under investigation, there is strong evidence that OPs are highly dependent on the maturation of the visual system (Westall et al., 1999; Moskowitz et al., 2005). In a mouse model of retinopathy of

prematurity, where the OPs were attenuated by 50%, compared to the control, a decrease in thickness of the inner plexiform layer, outer plexiform layer, and the inner nuclear layer was found, though, no damage to the ganglion cell layer was reported (Nakamura et al., 2012). This is indicative of evidence that ganglion cells may not be responsible for OP generation. Contrary to this finding, a correlation between decrease in fast OP RMS amplitude (obtained using fast sequence mfERG) and depreciation in ganglion cell density has been reported, with OP amplitude reaching near 0 μV as ganglion cell density reaches 0% of the control (Rangaswamy et al., 2006). In addition, slow response OPs (extracted in the 90 - 300 Hz range, by slowing the m-sequence presentation), are sensitive to tetrodotoxin (TTX), indicating a role of spiking retinal neurons in their generation (Rangaswamy et al., 2003). Ganglion cells and some amacrine cells are the only spiking neurons in the retina.

Evaluation of OPs using the meERG technique, which has a potential application to be used for clinical detection, diagnosis and monitoring of eye disease, may also provide further insight into the cellular origins of this high frequency ERG component. Combining the knowledge of vertical orientation of cells with the lateral distribution, the cellular activity can be localized. In topography studies of ganglion cell, the cell density has been reported to peak at 1mm (35,100 cells/mm^2) from the foveal center, and drops to much lower cellular density with increasing radial eccentricity (Curcio and Allen, 1990). Comparing this to the meERG, it would be expected to have a stronger OP response from the central electrodes (C ring and middle electrode) than the peripheral electrodes (A ring). Therefore, a disease state affecting the ganglion cells would most likely show an attenuated OP response in the central electrodes. Furthermore, Curcio and Allen (1990)

reported that there was substantial difference in the mean density of ganglion cells between individuals. In the current study, OP variation was analyzed between animals, there was a large difference found. This variability could be representative of the variation of the cellular density in the retinal makeup of the individual. Therefore, characterizing variance of the normative data is an essential step towards optimizing measurement and diagnosis, and differentiating disease state, and óabnormalô data.

It has also been reported that the ganglion cell layer also consists of displaced amacrine cells, the cellular density of which peaks between 2mm to 6mm (1,000 ï 1,200 cells/mm^2) from the foveal center and slowly declines to 650 cells/mm^2 at 18 mm (Curcio and Allen, 1990). Even though the number of the displaced amacrine cells is much lower than the ganglion cells, a disease state affecting the amacrine cells, may also show attenuation in the central meERG response. Since there are several different types of amacrine cells, with a variety of different functions, a disease may not affect all amacrine cells, and the OP response would vary. A better understanding of the cellular arrangement and topography, along with the meERG response, would allow assessing the variation in magnitude and/ or polarity of the recorded ERG response across the cornea and alteration of cellular current across the retina.

Oscillatory potentials have also been reported to be sensitive to alterations in sensitivity of the inner retinal layer in both rat models (Layton et al., 2007) and humans (Movasat et al., 2008). In further analysis of individual OP peaks, OP1 was most sensitive to diabetic retinopathy (DR), (Movasat et al., 2008). In DR disease model, OP2 (Movasat et al., 2008; Vessey et al., 2011) and OP3 (Movasat et al., 2008) are unaffected, compared to control. On the other hand, OP2 has been reported to be affected in patients

with age-related macular degeneration (AMD). The amplitude of OP4 has been reported to have correlation with vascular dysfunction (Luu et al., 2010). By using this knowledge of variations in individual OP peaks with the meERG, localized assessment of retinal damage due to specific disease states can be potentially inferred.

Oscillatory potentials remain of significance clinical importance (Speros and Price, 1981; Wachtmeister, 1998). The most widely studied disease state which is analyzed by ERG OPs has been diabetic retinopathy. With more understanding of OPs, they may be used as a measure of early detection of diabetic retinopathy (DR) (Vadala et al., 2002) and a sensitive diagnostic measure of progression of DR (Kizawa et al., 2006). The scotopic SOP amplitude has been reported as a promising non-invasive measure of early detection of glaucoma (Bayer et al., 2001). Furthermore, because of the sensitivity of OP measurement to DR disease state, they can be used to study the effect of treatment for DR (Fernandez et al., 2011; Nebbioso et al., 2012). OPs have also been used to assess the visual mechanism post surgery, such as for analysis of cystoids macular edema, reporting significant attenuation of OP amplitudes (Miyake et al., 1993; Terasaki et al., 2003).

VI. Conclusion

Because individual OP peaks vary with disease state, OPs have potential to be a diagnostic tool for multiple diseases. Standard guidelines on labeling, testing and reporting would be most useful. As has been the findings of this study, the stimulus strength varies the time and amplitude of OPs; it would important to classify the specific stimulus strength for clinical purposes in order to avoid artifactual delay and attenuation.

Since some peaks are excluded from analysis because of corruption due to other ERG components, the reporting method could be standardized by labeling all extracted peaks above a certain threshold. A peak excluded from analysis would also have its respective OP peak number. In addition, to make OPs standard for clinical use, light adaptation, measurement equipment and extraction parameters need to be consistent. Some of the inconsistencies and dissimilarity of results could be due to variation in range of filter passband frequencies.

These recommendations of standardizing OP recording and analysis using the meERG could be used to not only gain further understanding of the cellular origins of OPs, but also potentially be used as a measure of localized function and therefore diagnosis of multiple diseases causing damage to the retina.

VII. References

A.D.A.M Medical Encyclopedia (2011, September 26). Multiple Sclerosis. *PubMed Health*. Retrieved from http://www.ncbi.nlm.nih.gov/pubmedhealth/PMH0001747/

A.D.A.M. Medical Encyclopedia (2011, May 4). Retinopathy of Prematurity. *PubMed Health*. Retrieved from http://www.ncbi.nlm.nih.gov/pubmedhealth/PMH0002585/

A.D.A.M. Medical Encyclopedia (2011, September 14). Glaucoma. *PubMed Health*. Retrieved from http://www.ncbi.nlm.nih.gov/pubmedhealth/PMH0002587/

A.D.A.M. Medical Encyclopedia (2012, January 3). Diabetes and eye disease. *PubMed Health*. Retrieved from http://www.ncbi.nlm.nih.gov/pubmedhealth/PMH0002192/

Akula, J., Mocko, J., Moskowitz, A., Hansen, R., & Fulton, A. (2007). The Oscillatory Potentials of the Dark-Adapted Electroretinogram in Retinopathy of Prematurity. *Investigative Ophthalmology & Visual Science*, *48*(12), 5788-5797.

Asi, H., & Perlman, I. (1992). Relationships between the electroretinogram a-wave, b-wave and oscillatory potentials and their application to clinical diagnosis. *Documenta Ophthalmologica*, *79*(2), 125-139.

Bayer, A. U., Danias, J., Brodie, S., Maag, K. P., Chen, B., Shen, F., Mittag, T. W. (2001). Electrorinographic Abnormalities in a Rat Glaucoma Model with Chronic Elevated Intraocular Pressure. *Experimental Eye Research*, *72*, 667-677.

Bui, B. V., Armitage, J. A., & Vingrys, A. J. (2002). Extraction and modeling of oscillatory potentials. *Documenta Ophthalmologica*, *104*, 17-36.

Burstedt, M. S., Sandgren, O., Golovleva, I., & Wachtmeister, L. (2008). Effects of prolonged dark adaptation in patients with retinitis pigmentosa of Bothnia type: an electrophysiological study. *Documenta Ophthalmologica*, *116*(3), 193-205.

Chen, J. C., Brown, B., & Schmid, K. L. (2006). Evaluation of inner retinal function in myopia using oscillatory potentials of the multifocal electroretinogram. *Vision Research*, *46*(24), 4096-4103.

Cobb, W. A., & Morton, H. B. (1953). A new component of the human electroretinogram. *Proceedings of the Physiological Society*, *18*, 36-37.

Curcio, C. A., & Allen, K. A. (1990). Topography of Ganglion Cells in Human Retina. *Journal of Comparative Neurology*, *300*(1), 5-25.

Fernandez, D. C., Sande, P. H., Chianelli, M. S., Aldana Marcos, H. J., & Rosenstein, R. E. (2011). Induction of Ischemic Tolerance Protects the Retina From Diabetic Retinopathy. *The American Journal of Pathology, 178*(5), 2264-2275.

Forooghian, F., Kertes, P. J., & Aptsiauri, N. (2003). Probable autoimmune retinopathy in a patient with multiple sclerosis. *Canadian Journal of Ophthalmology, 38*(7), 593-597.

Forooghian, F., Sproule, M., Westall, C., Gordon, L., Jirawuthiworavong, G., Shimazaki, K., & O'Connor, P. (2006). Electroretinographic abnormalities in multiple sclerosis possible role for retinal autoantibodies. *Documenta Ophthalmologica, 113*, 123-132.

Fortune, B., Bearse, M. A., Cioffi, G. A., & Johnson, C. A. (2002). Selective Loss of an Oscillatory Component from Temporal Retinal Multifocal ERG Responses in Glaucoma. *Investigative Ophthalmology & Visual Science, 43*(8), 2638-2647.

Fujikado, T., Hosohata, J., & Omoto, T. (1996). ERG of form deprivation myopia and drug induced ametropia in chicks. *Current Eye Research, 15*(1), 79-86.

Fujikado, T., Kawasaki, Y., Suzuki, A., Ohmi, G., & Tano, Y. (2007). Retinal function with lens-induced myopia compared with form-deprivation myopia in chicks. *Graefe's Archive of Clinical Experimental Ophthalmology, 235*(5), 320-324.

Fulton, A. B., & Hansen, R. M. (1996). Photoreceptor function in infants and children with a history of mild retinopathy of prematurity. *Journal of the Optical Society of America,13*(3), 566-571.

Gorczyca, W. A., Ejma, M., Witkowska, D., Misiuk-Hojlo, M., Kuropatwa, M., Mulak, M., & Szymaniec, S. (2004). Retinal antigens are recognized by antibodies present in sera of patients with multiple sclerosis. *Ophthalmic Research, 36*(2), 120-123.

Gundogan, F. C., Erdurman, C., Durukan, A. H., Sobaci, G., & Bayraktar, M. Z. (2007). Acute effects of cigarette smoking on multifocal electroretinogram. *Clinical and Experimental Ophthalmology, 35*, 32-37.

Hancock, H. A., & Kraft, T. W. (2004). Oscillatory Potential Analysis and ERGs of Normal and Diabetic Rats. *Investigative Ophthalmology & Visual Science, 45*(3), 1002-1008.

Hancock, H. A., & Kraft, T. W. (2008). Human oscillatory potentials: intensity-dependence of timing and amplitude. *Documenta Ophthalmologica, 117*, 215-222.

Hassan-Karimi, H., Jafarzadehpur, E., Blouri, B., Hashemi, H., Sadeghi, A. Z., Mirzajani, A. (2008). Frequency Domain ERG in Retinitis Pigmentosa versus Normal Eyes. *Journal of Ophthalmic & Vision Research, 7*(1), 34-38.

Heiduschka, P., Julien, S., Schuettauf, F., & Schnichels, S. (2010). Loss of retinal function in aged DBA/2J mice - New insights into retinal neurodegeneration. *Experimental eye research, 91*(5), 779-783.

Hood, D. C., & Birch, D. G. (1996). b wave of the scotopic (rod) electroretinogram as a measure of the activity of human on-bipolar cells. *Journal of the Optical Society of America A, 13*(3), 623-633.

Hood, D. C., Frishman, L. J., Saszik, S., & Viswanathan, S. (2002). Retinal Origins of the Primate Multifocal ERG: Implications for the Human Response. *Investigative Ophthalmology & Visual Science, 43*(5), 1673-1685.

Huber, M., Heiduschka, P., Ziemssen, F., Bolbrinker, J., & Kreutz, R. (2011). Microangiopathy and visual deficits characterize the retinopathy of a spontaneously hypertensive rat model with type 2 diabetes and metabolic syndrome. *Hypertension Research, 34*, 103-112.

Ikenoya, K., Kondo, M., Piao, C. H., Kachi, S., Miyake, Y., & Teraski, H. (2007). Preservation of macular oscillatory potentials in eyes of patients with retinitis pigmentosa and normal visual acuity. *Investigative Ophthalmology & Visual Science, 48*(7), 3312-3317.

Ingenito, A. J. (1979). Effects of cigarette smoke inhalation on the cat electroretinogram: comparisons with nicotine and carbon monoxide. *Journal of Pharmacology & Experimental Therapeutics, 211*(3), 647-655.

Kaneko, A. (1970). Physiological and morphological identification of horizontal, bipolar and amacrine cells in goldfish retina. *Journal of Physiology, 207*, 623-633.

Karwoski, C. J., Xu, X., & Yu, H. (1996). Current-source density analysis of the electroretinogram of the frog: methodological issues and origin of components. *Journal of the Optical Society of America A, 13*(3), 549-556.

Kellogg Eye Center - University of Michigan (2012). Cystoid Macular Edema (CME). *Patient Care Eye Conditions*. Retrieved from http://www.kellogg.umich.edu/patientcare/conditions/cystoid.macular.edema.html

Kergoat, H. Kergoat MJ., Justino L. (2001). Age-related changes in the flash electroretinogram and oscillatory potentials in individuals age 75 and older. *Journal of American Geriatric Society, 49*(9), 1212-1217

Kizawa, J., Machida, S., Kobayashi, T., Gotoh, Y., & Kurosaka, D. (2006). Changes of Oscillatory Potentials and Photopic Negative Response in Patients with Early Diabetic Retinopathy. *Japan Journal of Ophthalmology, 50*, 367-373.

Kojima, M., & Zrenner, E. (1978). Off-components in response to brief light flashes in the oscillatory potential of the human electroretinogram. *Albrecht Von Graefe's Archive of Clinical Experimental Ophthalmology, 206*(2), 107-120.

Lachapelle, P. (1990). Oscillatory Potentials as predictors to amplitude and peak time of the photopic b-wave of the human electroretinogram. *Documenta Ophthalmologica, 75*, 73-82.

Layton, C. J., Safa, R., & Osborne, N. N. (2007). Oscillatory potentials and the b-Wave: Partial masking and interdependence in dark adaptation and diabetes in the rat. *Graefe's Archive of Clinical Experimental Ophthalmology, 245,* 1335-1345.

Lei, B., Yao, G., Zhang, K., Hofeldt, K. J., & Chang, B. (2006). Study of rod- and cone-driven oscillatory potentials in mice. *Investigative Ophthalmology & Visual Science, 47*(6), 2732-2738.

Leighton, D. A., Bhargava, S. K., & Shail, G. (1979). Tobacco Amblyopia: The Effect of Treatment on the Electroretinogram. *Documenta Ophthalmologica*, *46*(2), 325-331.

Liu, K., Akula, J., Hansen, R., Moskowitz, A., Kleinman, M., & Fulton, A. (2006). Development of the Electroretinogram Oscillatory Potentials in Normal and ROP Rats. *Investigative Ophthalmology & Visual Science*, *47*(15), 5447-5451.

Luu, C. D., Szental, J. A., Lee, S., Lavanya, R., & Wong, T. Y. (2010). Correlation between Retinal Oscillatory Potentials and Retinal Vascular Caliber in Type 2 Diabetes. *Investigative Ophthalmology & Visual Science*, *51*(1), 482-486.

Marmor, M. F., Fulton, A. B., Holder, G. E., Miyake, Y., Brigell, M., & Bach, M. (2009). ISCEV Standard for full-field clinical electroretinography (2008 update). *Documenta Ophthalmologica*, *118*, 69-77.

Mecklenburg, J., Clancy, E. A., & Tzekov, R. (2011). Automated Oscillatory Potential Detection and Parameter Extraction in the Electroretinogram. *IEEE 27th Annual Northeast Bioengineering Conference, 1-3 April, 2011*.

Miyake, Y., Miyake, K., & Shiroyama, N. (1993). Classification of aphakic cystoid macular edema with focal macular electroretinograms. *American Journal of Ophthalmology*, *116*(5), 576-583.

Moskowitz, A., Hansen, R., & Fulton, A. (2005). ERG oscillatory potentials in infants. *Documenta Ophthalmologica*, *110*, 265-270.

Movasat, M., Modarresi, M., Mansouri, M., Nilli-AhmadAbadi, M., & Rajabi, M. (2008). Oscillatory Potentials in Diabetic Retina without Retinopathy. *Iranian Journal of Ophthalmology*, *20*(1), 20-24.

Nakamura, S., Imai, S., Ogishima, H., Tsuruma, K., Shimazawa, M., & Hara, H. (2012). Morphological and Functional Changes in the Retina after Chronic Oxygen-Induced Retinopathy. *PLoS ONE, 7*(2).

National Eye Institute. (2009). Facts About Age-Related Macular Degeneration. *National Eye Institute*. Retrieved from http://www.nei.nih.gov/health/maculardegen/armd_facts.asp

Nebbioso, M., Federici, M., Rusciano, D., Evangelista, M., & Pescosolido, N. (2012). Oxidative Stress in Preretinopathic Diabetes Subjects and Antioxidants. *Diabetes Technology & Therapeutics*, *14*(3), 257-263.

Nork, T. M., Poulsen, G. L., Nickells, R. W., Ver Hoeve, J. N., Cho, N. C., Levin, L. A., & Lucarelli, M. J. (2000). Protection of ganglion cells in experimental glaucoma by retinal laser photocoagulation. *Archive of Ophthalmology*, *118*(9), 1242-1250.

O'Donnell, M., & Talbot, J. F. (1987). Vitamin A deficiency in treated cystic fibrosis: case report. *British Journal of Ophthalmology, 71*, 787-790.

Palmowski-Wolfe, A. M., Todorova, M. G., & Orgul, S. (2011). Multifocal Oscillatory Potentials in the 'Two Global Flash mfERG in High and Normal Tension Primary Open-Angle Glaucoma. *Journal of Clinical Experimental Ophthalmology*, *2*(6), 1-5.

Rangaswamy, N. V., Hood, D. C., & Frishman, L. J. (2003). Regional variations in local contributions to the primate photopic flash ERG: revealed using the slow-sequence mfERG. *Investigative Ophthalmology & Visual Science*, *44*(7), 3233-3247.

Rangaswamy, N. V., Zhou, W., Harwerth, R. S., & Frishman, L. J. (2006). Effect of Experimental Glaucoma in Primates on Oscillatory Potentials of the Slow-Sequence mfERG. *Investigative Ophthalmology &Visual Science, 47*(2), 753-767.

Ruether, K., Grosse, J., Matthiessen, E., Hoffmann, K., & Hartmann, C. (2000). Abnormalities of the photoreceptor - bipolar cell synapse in a substrain of C57BL/10 mice. *Investigative Ophthalmology & Visual Science*, *41*, 4039-4047.

Sakai, T., Kondo, M., Ueno, S., Koyasu, T., Komeima, K., & Terasaki, H. (2009). Supernormal ERG oscillatory potentials in transgenic rabbit with rhodopsin P347L mutation and retinal degeneration. *Investigative Ophthalmology & Visual Science*, *50*(9), 4402-4409.

Severns, M. L., Johnson, M. A., & Bresnick, G. H. (1994). Methodologic dependence of electroretinogram oscillatory potential amplitudes. *Documenta Ophthalmologica*, *86*, 23-31.

Speros, P., & Price, J. (1981). Oscillatory Potentials. History, Techniques and Potential Use in the Evaluation of Disturbances of Retinal Circulation. *Survey of Ophthalmology*, *25*(4), 237-252.

Steinberg, R. H. (1966). Oscillatory activity in the optic tract of cat and light adaptation. *Journal of Neurophysiology*, *29*(2), 139-156.

Suttle, C. M., & Harding, G. F. (1998). The VEP and ERG in a young infant with cystic fibrosis. *Documenta Ophthalmologica*, *95*(1), 63-71.

Terasaki, H., Miyake, K., & Miyake, Y. (2003). Reduced oscillatory potentials of the full-field electroretinogram of eyes with aphakic or pseudophakic cystoid macular edema. *American Journal of Ophthalmology*, *135*(4), 477-482.

Van der Torren, K. K., Groeneweg, G. G., & Van Lith, G. G. (1988). Measuring oscillatory potentials: Fourier analysis. *Documenta Ophthalmologica*, *69*(2), 153-159.

Vandala, M., Anastasi, M., Lodato, G., & Cillino, S. (2002). Electroretinographic oscillatory potentials in insulin-dependent diabetes patients: A long-term follow-up. *Acta Ophthalmologica Scandinavica*, *80*, 305-309.

Varghese, S. B., Reid, J. C., Hartmann, E. E., & Keyser, K. T. (2011). The Effect of Nicotine on the Human Electroretinogram. *Investigative Ophthalmology & Visual Science*, *52*(13), 9445-9451.

Vessey, K. A., Wilkinson-Berka, J. L., & Fletcher, E. L. (2011). Characterization of Retinal Function and Glial Cell Response in a Mouse Model of Oxygen-Induced Retinopathy. *The Journal of Comparative Neurology*, *519*, 506-527.

Wachtmeister, L. (1998). Oscillatory Potentials in the Retina: what do they reveal. *Progress in Retinal and Eye Research*, *17*(4), 485-521

Wachtmeister, L., & Dowling, J. E. (1978). The oscillatory potentials of the mudpuppy retina. *Investigative Ophthalmology & Visual Science*, *17*, 1176-1188.

Walters, P., Widder RA., Lüke C., Königsfeld P., Brunner R. (1999). Electrophysiological abnormalities in age-related macular degeneration. *Graefe's Archive of Clinical Experimental Ophthalmology. 237*(12), 962-968.

Westall, C. A., Dhaliwal, H. S., Panton, C. M., Sigesmun, D., Levin, A. V., Nischal, K. K., & Heon, E. (2001). Values of electroretinogram responses according to axial length. *Documenta Ophthalmologica*, *102*(2), 115-130.

Westall, C. A., Panton, C. M., & Levin, A. V. (1999). Time courses for maturation of electroretinogram responses from infancy to adulthood. *Documenta Ophthalmologica*, *96*(4), 355-379.

Whatham, A., Suttle, C., Blumenthal, C., Allen, J., & Gaskin, K. (2009). ERGs in children with pancreatic enzyme insufficient and pancreatic enzyme sufficient cystic fibrosis. *Documenta Ophthalmologica*, *119*, 43-50.

Zhou, X., Huang, X., Chen, H., & Zhao, P. (2010). Comparison of electroretinogram between healthy and preterm infants. *Documenta Ophthalmologica*, *121*, 205-2

VIII. Appendix I

Test to examine if the filter is working properly:

A series of sine waves with different frequencies were passed through the 4th order Butterworth filter, with a highpass cutoff of 100 Hz and a lowpass cutoff of 300 Hz.

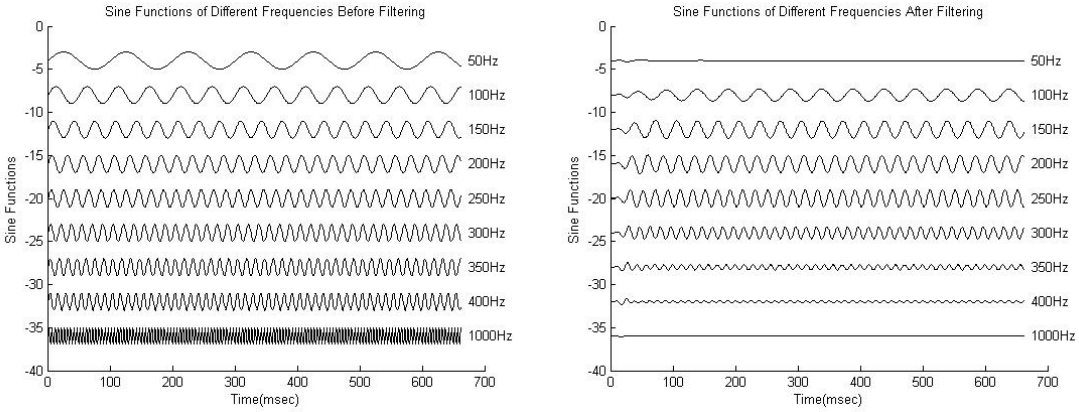

Comparison of 2nd and 4th order Butterworth filter at 100 ï 300 Hz bandwidth:

Shifting from 2nd to 4th order filtering does not seem to affect the third peak in the series. However, all other peaks in the 2nd order filter are delayed.

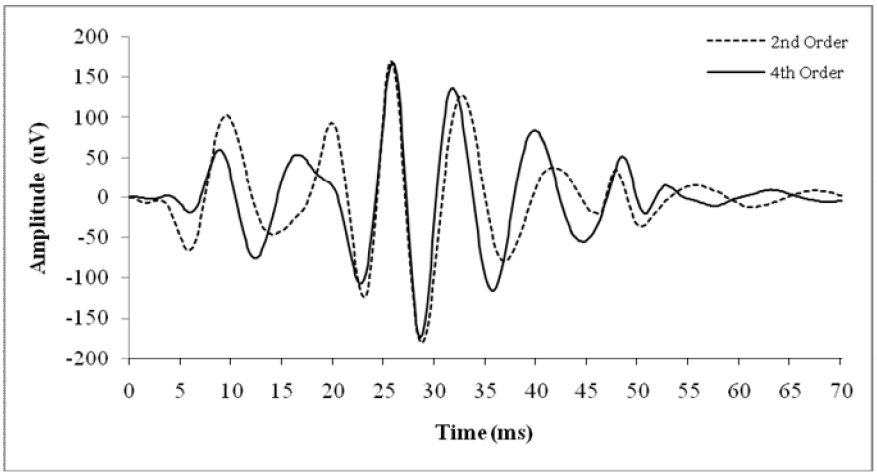

Comparison of different highpass cutoff frequencies for the 4th order Butterworth filter:

It can be seen that not only does the cutoff frequency modify the amplitude of the peaks and their implicit times, but it also affects the number of peaks generated from the specific ERG signal. Marmor et al. (2004) have reported in the ISCEV guidelines that the type of filter can cause phase shift and ringing or the OPs.

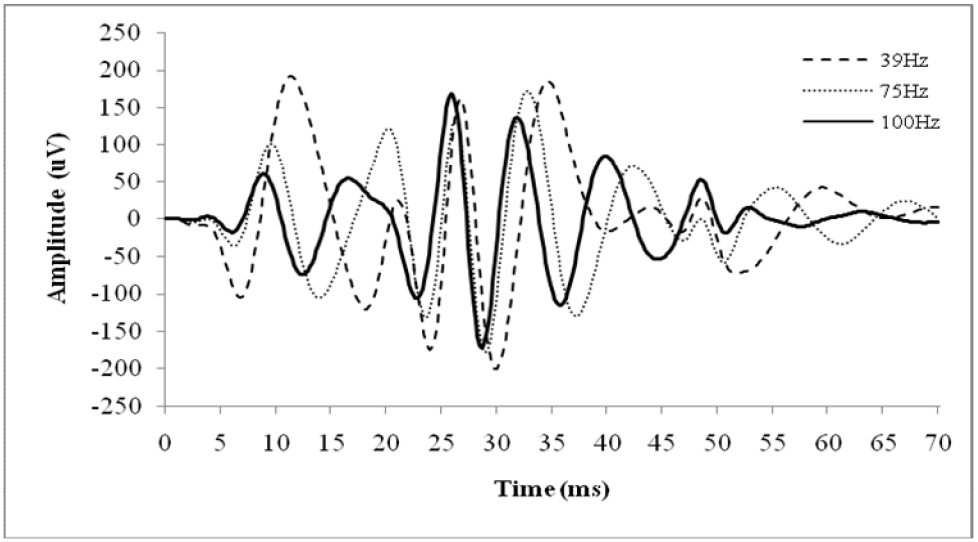

Comparison of evaluation of amplitudes using the sum of peaks method and root mean square of the amplitudes:

Sum of Peaks measurement was used to do the analysis in this study. The analysis can also be done using Root Mean Square. Calculations done for OP data from different electrodes on the lens resulted in approximately the same result for either SOP or RMS method. Some of the comparison calculation examples are shown below.

Electrode Number	Electrode Ring Number	Sum of Peaks	Root Mean Square
E73	A1	913.06	82.34
E83	A2	899.02	81.17
E64	A3	904.40	81.50
E74	A4	888.35	79.98
E53	A5	904.89	81.37
E54	A6	1699.97	132.88
E61	A7	895.39	80.66
E62	A8	884.30	79.65
E78	A9	881.87	79.51
E66	A10	899.06	80.97
E87	A11	905.37	81.65
E82	A12	913.40	82.43
E86	B1	923.66	83.20
E65	B2	915.59	82.55
E75	B3	899.46	81.08
E55	B4	1797.86	144.89
E67	B5	895.93	80.78
E71	B6	902.93	81.30
E63	B7	909.29	81.95
E72	B8	918.42	82.76
E76	C1	921.90	83.28
E51	C2	919.20	82.63
E68	C3	1737.88	139.94
E77	C4	907.20	81.86
E56	M	914.90	82.51

Comparison between SOP and RMS

$$\frac{(SOP_1 - SOP_2)}{((SOP_1 + SOP_2)/2)} = \frac{(RMS_1 - RMS_2)}{((RMS_1 + RMS_2)/2)}$$

Examples:

Left and Right: A12 and A4

SOP	RMS
0.02781	0.03016

Left and Middle: A12 and M

SOP	RMS
-0.00165	-0.00087

Top and Bottom: B1 and B7

SOP	RMS
0.01568	0.01515

Top and Middle: B1 and M

SOP	RMS
0.009528	0.00838

IX. Appendix II

Data Table for Figure 25

Stimulus (sc cd s/m^2)	Log Stimulus (sc cd s/m^2)	Average	Standard Deviation
0.01	**-2.00**	204.91	1.21
5.84	**0.77**	140.20	0.00
19.98	**1.30**	136.68	0.13
30.4	**1.48**	133.39	0.04
73.4	**1.87**	123.45	0.09
116.4	**2.07**	117.34	0.10
159.0	**2.20**	113.98	0.06

Data table for Figure 26

Stimulus (sc cd s/m^2)	**0.01**	**5.841**	**19.98**	**30.4**	**73.4**	**116.4**	**159**
log Stimulus (sc cd s/m^2)	**-2.000**	**0.766**	**1.301**	**1.483**	**1.866**	**2.066**	**2.201**
Average of OP1	40.800	24.000	23.000	23.000	18.045	17.136	16.582
Average of OP2	48.127	31.600	30.800	29.800	28.200	26.600	25.800
Average of OP3	52.882	38.200	37.100	36.000	34.400	32.600	31.800
Average of OP4	63.100	46.400	45.782	44.591	42.800	41.000	39.800
Std. Deviation of OP1	0.175	0	0	0	0.086	0.095	0.059
Std. Deviation of OP2	0.098	0	0	0	0	0	0
Std. Deviation of OP3	0.300	0	0.102	0	0	0	0
Std. Deviation of OP4	0.816	0	0.059	0.043	0	0	0

Data table for Figure 27

Stimulus (sc cd s/m^2)	Log Stimulus (sc cd s/m^2)	Average	Standard Deviation
0.01	**-2.00**	434.33	9.58
5.84	**0.77**	474.76	4.50
19.98	**1.30**	829.08	8.82
30.4	**1.48**	863.68	11.64
73.4	**1.87**	859.81	10.49
116.4	**2.07**	928.89	10.80
159	**2.20**	905.35	11.76

Data table for Figure 28

Stimulus (sc cd s/m^2)	**0.01**	**5.841**	**19.98**	**30.4**	**73.4**	**116.4**	**159**
log Stimulus (sc cd s/m^2)	**-2.00**	**0.77**	**1.30**	**1.48**	**1.87**	**2.07**	**2.20**
Average of OP1	13.11	19.15	33.77	54.52	72.46	103.80	128.27
Average of OP2	84.24	91.43	254.52	270.98	267.97	288.94	272.05
Average of OP3	235.87	188.49	335.76	342.42	324.84	335.33	306.28
Average of OP4	89.95	175.69	205.04	195.76	194.54	200.82	198.74
Std. Deviation of OP1	0.94	0.79	0.85	1.08	1.34	1.26	2.15
Std. Deviation of OP2	12.14	1.58	3.32	3.57	3.08	3.24	3.11
Std. Deviation of OP3	49.94	2.63	4.62	4.84	4.41	4.41	4.57
Std. Deviation of OP4	13.90	2.60	2.97	2.68	2.32	2.45	2.83

VITA

NAME Maryam Hanif

EDUCATION

M.S. Bioengineering, (Concentration: Neural Engineering) July, 2012
University of Illinois at Chicago (UIC), Chicago, IL

B.S. Bioengineering, (Cell/Tissue Engineering) December, 2009
University of Illinois at Chicago (UIC), Chicago, IL

EXPERIENCE

01/11 to Present — Neural Engineering Vision Lab, UIC — Chicago, IL
Graduate Researcher; Advisor: Dr. John R. Hetling

- Signal processing: multi-electrode Electroretinogram (meERG)
- Evaluate oscillatory potentials in normative data for further analysis of eye disease detection using the meERG

08/10 ï 05/11 — University of Illinois at Chicago — Chicago, IL
Graduate Teaching Assistant

- Courses: Biostatistics, Neural Engineering Lab

05/10 ï 08/10 — Medtronic, Inc. ï Ventures and New Therapies Dept. — Fridley, MN
Engineering Associate Intern

- Evaluate effect of photosensitizers on cancer cell lines
- Set up matrixed experiments; cell culture, conduct assays, staining/imaging
- Suggested a new compound, that was very effective in initial experiments

08/07 ï 05/09 — University of Illinois at Chicago — Chicago, IL
Undergraduate Researcher

- Levitan Lab ï Develop 3D constructs to mimic i*n-vivo* environment to effectively differentiate hESCs (human Endothelial Stem Cells) into Endothelial Cells ï Established 77% differentiation
- Mahmud Lab ï Study markers of Hematopoietic cells ï Cell culture
- Orjala Lab ï Evaluate cytotoxicity of natural pharmaceutical compounds
  - Operate HPLC; Make crude extracts; Fractionation
- Eddington Lab ï Study surface properties of biomaterial ï polydimethylsiloxane (PDMS)
  - Operate plasma system; Develop PDMS

08/07 ï 12/07 — Oakton Community College — Des Plaines, IL
Student Researcher; Advisor: Gary Mines

- Study invasiveness of plant species in the Midwest
- Design experimental protocol to test plant invasiveness

08/07 ï 12/07 Oakton Community College Des Plaines, IL

Assistant to the Honors Program Coordinator

- Process and mail information related to the program
- Assist students with Honors Program inquiries

SKILLS

Instruments: Electron Microscopy, High Performance Liquid Chromatography (HPLC)
Software: MATLAB
Languages: English, Hindi/Urdu
Coursework: Medical device development requirements (FDA/ ISO), Risk assessment

ACTIVITIES

2012 ð *Volunteer* ï World Summit of Nobel Laureates ï (Chicago, 2012)
08/11 ï present ð *Director* ï Cell/Tissue Engineering Lab Learning Program
08/09 ï present ð *Department Representative (Bioengineering)* ï Graduate Student Council
08/08 ï present ð *Student Body Representative* ï Chancellorôs Committee on the Status of Women
08/09 ï 01/12 ð *Advisory Board / Reviewer* ï UIC Bioengineering Journal
08/07 ï 05/11 ð *Mentor* ï Women in Science and Engineering (WISE)
08/10 ï 12/10 ð *Volunteer* ï Chicago Lighthouse for Blind and Visually Impaired
05/10 ï 08/10 ð *Volunteer (student)* ï Emergency Response Team (at Medtronic, Inc.)
08/08 ï 05/09 ð *Co-President* ï Society of Women Engineers (SWE)
08/07 ï 08/08 ð *Editor and Writer* ï OCCurence (Oakton College School Newspaper)
01/06 ï 06/06 ð *Volunteer* ï Teaching Adults Program

MEMBERSHIP

08/08 ï present ð Tau Beta Pi
08/08 ï present ð Society of Women Engineers (SWE)
01/07 ï present ð National Society of Collegiate Scholars (NSCS)
01/07 ï 05/08 ð Engineering Council
08/07 ï 05/08 ð Science, Technology Engineering and Mathematics (STEM) Club

SCHOLARSHIPS AND ACHIEVEMENTS

ð GEM Fellowship (Medtronic, Inc. & UIC) ï Masters Education
ð Wentcher Scholarship (4 years) ï Bachelors Education
ð Union League of Chicago Engineerôs Foundation Scholarship (4 years)
Invited Speaker (Alumnus) ï 2009
ð Northrop Grumman/WISE Scholarship
ð University of Illinois Chicago College of Engineering Scholarship
ð Chancellorôs Student Service Award (2 years)